A novel energy-motion model for continuous sEMG decoding: from muscle energy to motor pattern

Gang Liu [1], Lu Wang [2], and Jing Wang [2]

[1]Xian Jiao Tong University
[2]Affiliation not available

October 30, 2023

Abstract

Myoelectric prosthetic hands create the possibility for amputees to control their prosthetics like native hands. However, user acceptance of the extant myoelectric prostheses is low. Unnatural control, lack of sufficient feedback, and insufficient functionality are cited as primary reasons. Recently, although many multiple degrees-of-freedom (DOF) prosthetic hands and tactile-sensitive electronic skins have been developed, no non-invasive myoelectric interfaces can decode both forces and motions for five-fingers independently and simultaneously. This paper proposes a myoelectric interface based on energy allocation and fictitious forces hypothesis by mimicking the natural neuromuscular system. The energy-based interface uses a kind of continuous "energy mode" in the level of the entire hand. According to tasks itself, each energy mode can adaptively and simultaneously implement multiple hand motions and exerting continuous forces for a single finger. Also, a few learned energy modes could extend to the unlearned energy mode, highlighting the extensibility of this interface. We evaluate the proposed system through off-line analysis and operational experiments performed on the expression of the unlearned hand motions, the amount of finger energy, and real-time control. With active exploration, the participant was proficient at exerting just enough energy to five fingers on "fragile" or "heavy" objects independently, proportionally, and simultaneously in real-time. The main contribution of this paper is proposing the bionic energy-motion model of hand: decoding a few muscle-energy modes of the human hand (only ten modes in this paper) map massive tasks of bionic hand.

Title

- A novel energy-motion model for continuous sEMG decoding from muscle energy to motor pattern

SUPPLEMENTARY MATERIALS

The PDF file includes:

Other Supplementary Material for this manuscript includes the following:

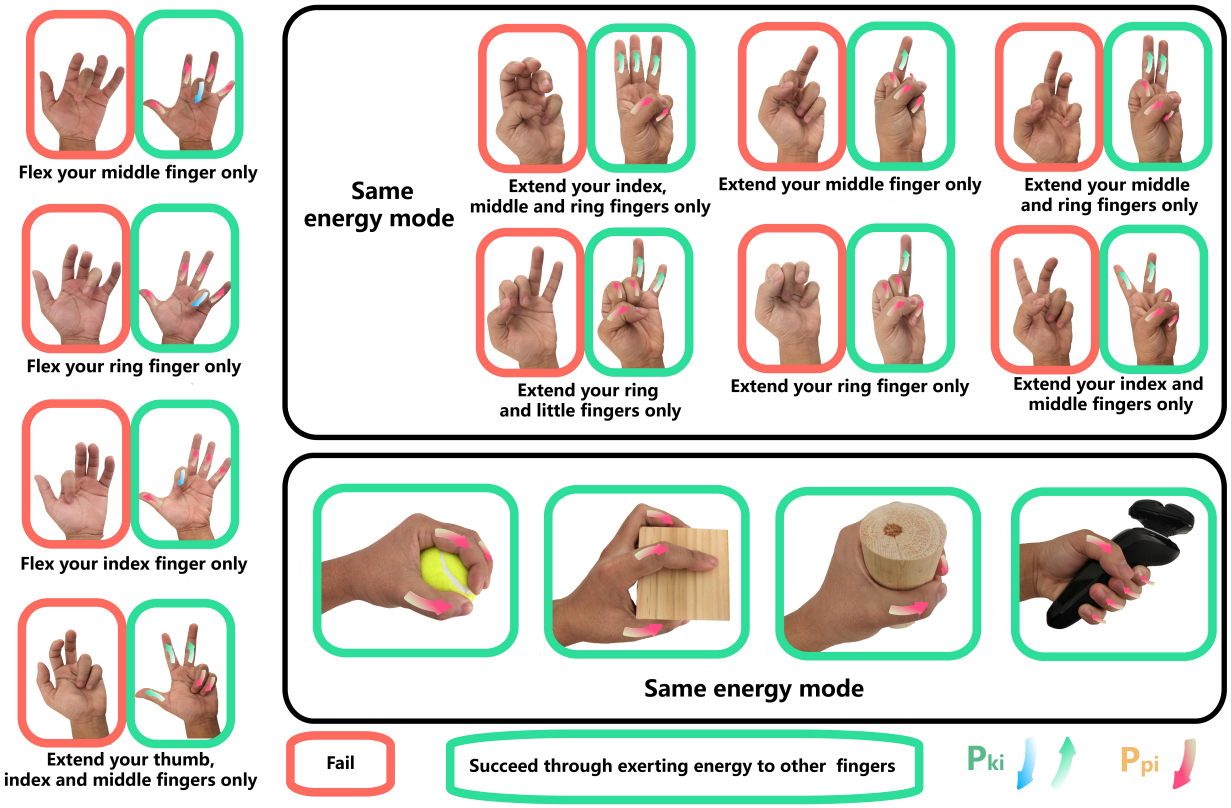

Fig. S1. The primary mechanism of human hand mimicked in the present study. We sought to regard the whole manual task as energy transfer, mimicking the adaptive mechanism of the human hand. The direction of arrows indicates "the direction of energy", and the same direction for five-fingers means that these hand motions could be achieved by the same energy mode. P_{ki} expresses the kinetic energy of the i-th finger, while P_{pi} expresses the potential energy of the i-th finger.

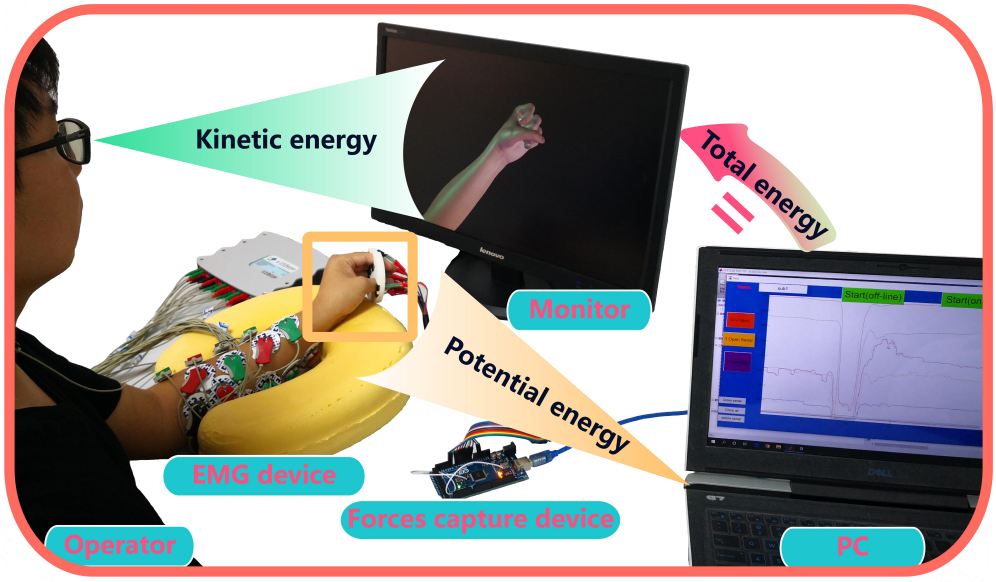

Fig. S2. Hardware structure for training states. The example of a hardware structure is composed of an EMG device, forces capture device, a PC, and a monitor. Note that, in the application, a smaller and general structure could achieve the frame of the myoelectric interface: electrodes, a microcomputer, and a motor unit.

EMG recording: Eight pairs of Ag-AgCl surface bipolar electrodes (interelectrode distance: average 3 mm) were placed on the subject's forearm to detect Surface EMG signals. Also, a single electrode was placed on the subject's to the left collarbone to serve as a ground and reference electrode. The positions of target muscles were mostly determined by palpation and the 3D-anatomical model in the experiments. The signals were sampled at 2400 Hz using four commercial 16-channel amplifiers (g.tec, Graz, Austria). Signals were band-pass filtered from 5 Hz to 500 Hz with an 8th order Chebyshev filter and a notch filter with a null frequency of 50 Hz, to ensure rejection of the 50 Hz power supply frequency. Data were recorded in MATLAB R2017b (The MathWorks, Massachusetts, USA). The software used to register the EMG signals has been programmed in Matlab Development Environment (The Mathworks Inc., Natick MA) using the API (Application Programming Interface) provided by the manufacturer (gUSBamp MATLAB API).

potential energy that converted into internal energy of the capture device proportional to forces (Finger forces recording): A fingertip force capture device that allows a simultaneous record of five-fingers forces is assembled. The capture device consists of an additional system (potential energy of each finger is converted into internal energy of the system), ten pressure sensors (RP-C7.6-LT, legact, China), and a microcontroller (Arduino Mega 2560, Arduino). The additional system was made of 3D printed polylactic acid (PLA). Ten pressure sensors were secured to each finger-hole of the additional system using tape. Specifically, each finger-hole was designed with two pressure sensors for the flexion and extension of the finger. The finger forces signals were sampled at 130 Hz and were digitized by the microcontroller with 10-bit precision. Finally, data were collected in MATLAB R2017b.

kinetic energy equaled to potential energy for each finger(Visual feedback): Visual feedback of the performed finger task was provided to the subjects using a computer graphic avatar body. The scene, displayed onto an LCD monitor, was

rendered from the virtual avatar, and the monitor was positioned in order to match the subject's perspective. The movement executed by the virtual hand was flexion and extension of the five-fingers congruent with the illusory movement that was expected by the finger motions (kinetic energy) of biological hand. The visual hand was developed with the Unity 3D game engine (Unity Technologies, San Francisco, USA).

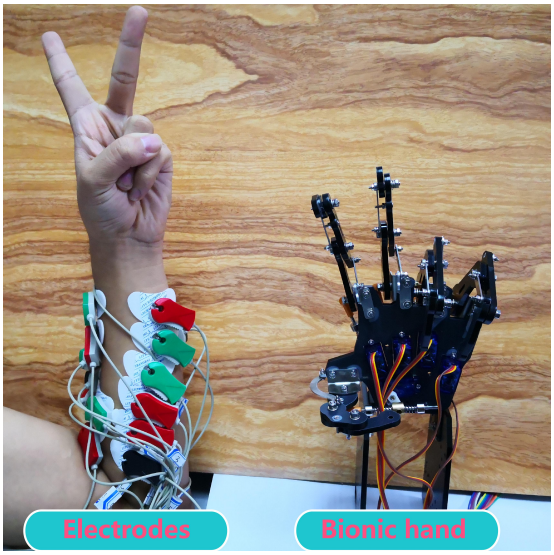

Fig. S3. Hardware structure for the application. The frame consists of electrodes, pc (in the back), and bionic hand.

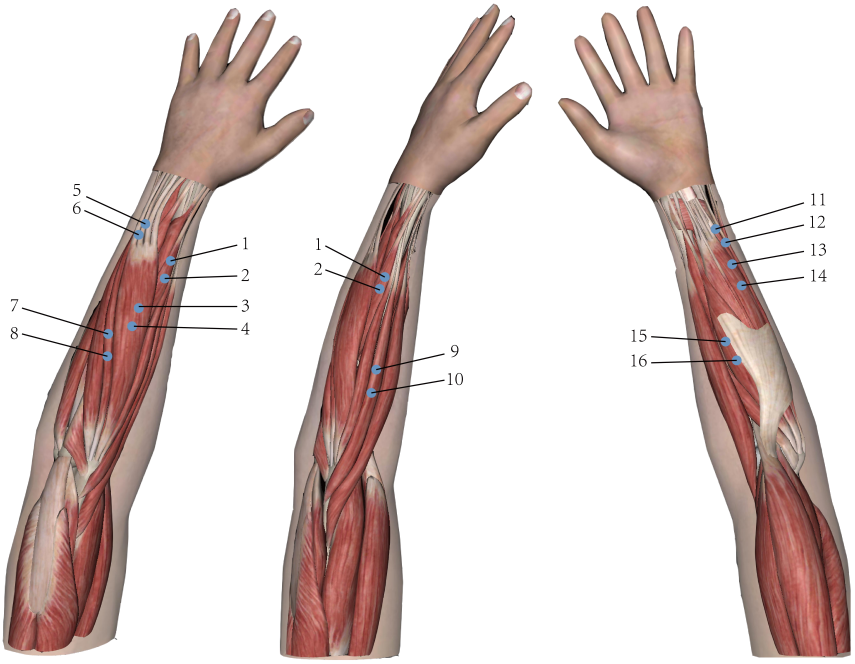

Fig. S4. EMG placement. Abductor pollicis longus (1,2): thumb abduction; Extensor digitorum (3,4): 2-5th finger extension; Extensor indicis (5,6): index finger; Extensor digiti minimi (7,8): little finger; Extensor carpi radialis longus (9,10): Wrist and thumb; Flexor digitorum profundus (11,12): 2-5th finger flexion; Flexor digitorum superficialis (13,14): 2-5th finger flexion; Flexor carpi radialis (15,16): Wrist and thumb;

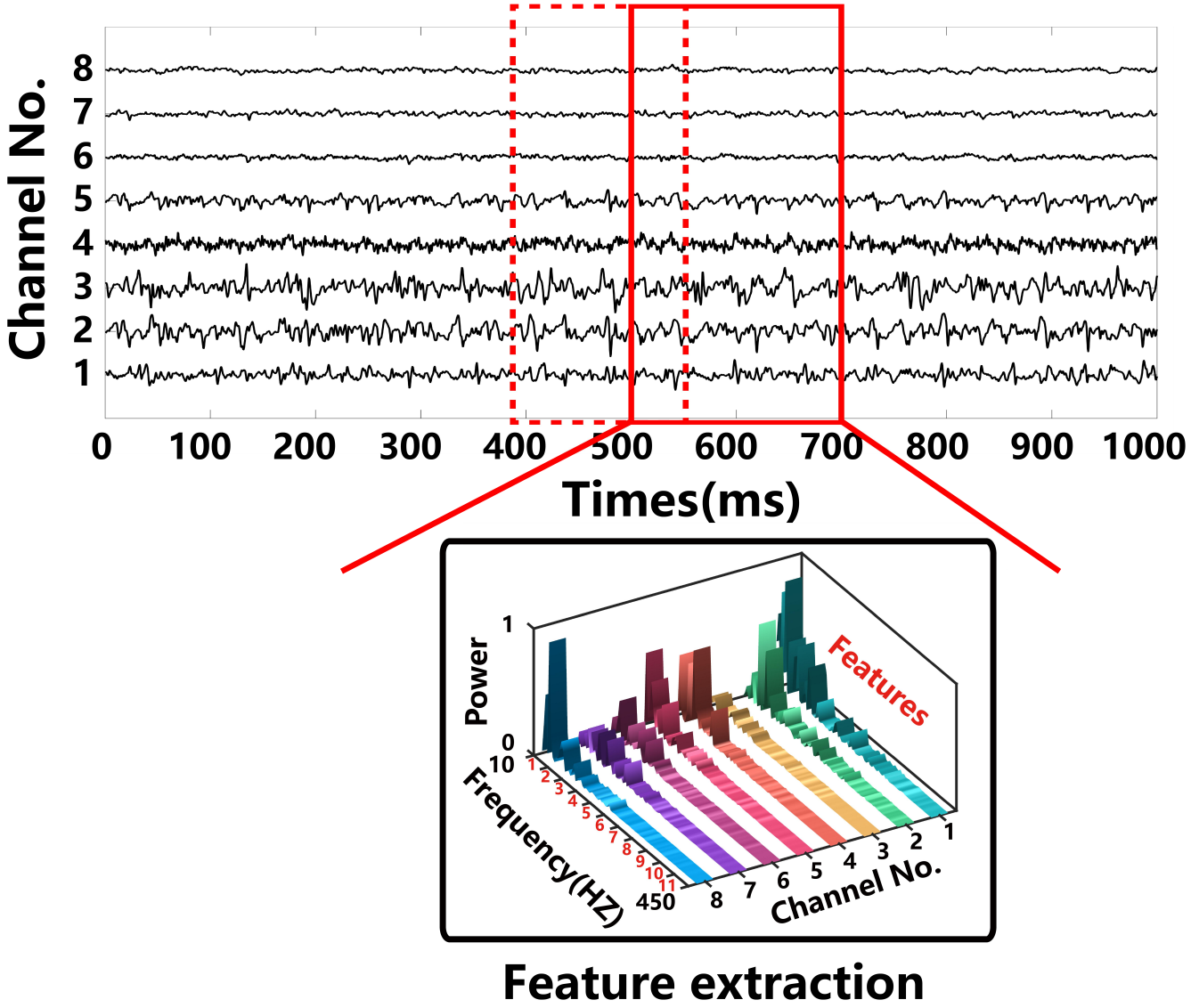

Fig. S5. Feature extraction by simple frequency-domain power. EMG amplitude is a simple and useful feature, as evidenced by commercial prostheses. To further improve the robustness to noise distinguishable by frequency band, we extract the frequency-domain power as features with a sample short-time Fourier transform, similar to amplitude in the different frequency band. Frequency bands encompassing the muscle (10–450 Hz) activities were created separately within each window. Each band was divided into 11 frequency bands (10-60HZ,60-100HZ,100-140HZ, etc.). The power across the selected frequency bands in each channel in the 200 ms sliding windows with 50 ms overlap were summed to produce 88 power features (11 features×8 channels).

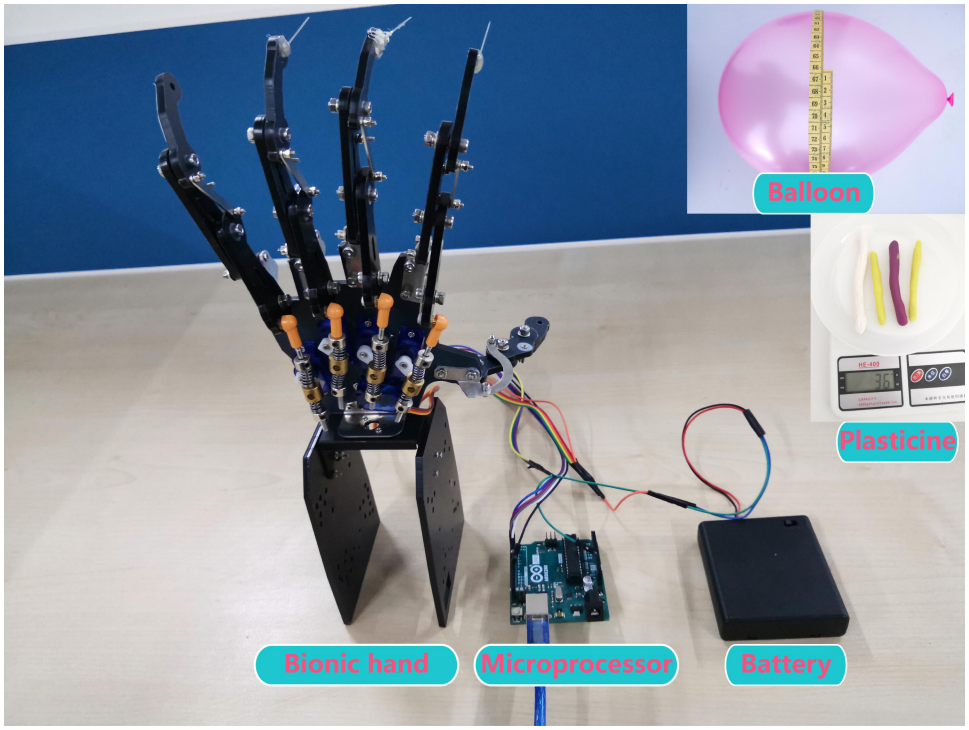

Fig. S6. Material for experiment 2 and experiment 3. Experiment 2: To test the degree to which the energy-based interface controls the amount of finger energy, we had the participant repeatedly perform these selected hand motions by controlling a bionic hand whose fingertips were fitted with steel needles, while ensuring breaking/non-breaking the balloon. Experiment 3: To assess the degree to control the finger energy in real-time, we had the participant repeatedly punch a hole in the plasticine (~1mm thickness) attached to the fixed balloon by using single fingers, while not breaking the balloon.

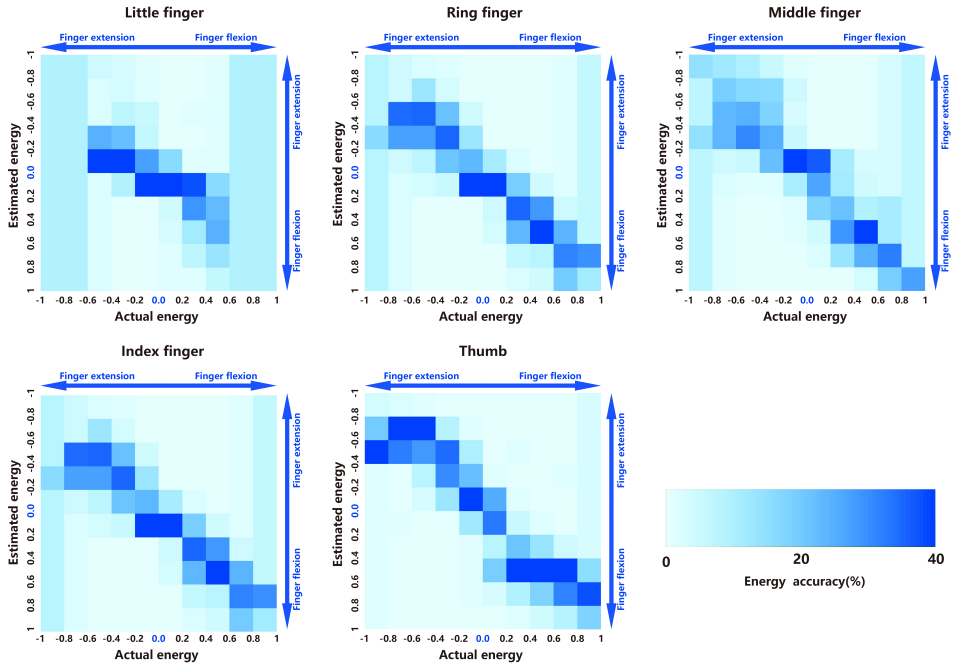

Fig. S7. Accuracy for the estimation of finger energy. Example of confusion matrix for the estimation of normalized finger energy (subject 4). Energy accuracy is defined as a ratio of the number of times within a certain energy interval to the total times. The confusion matrix shows some deviations similar to the native hand.

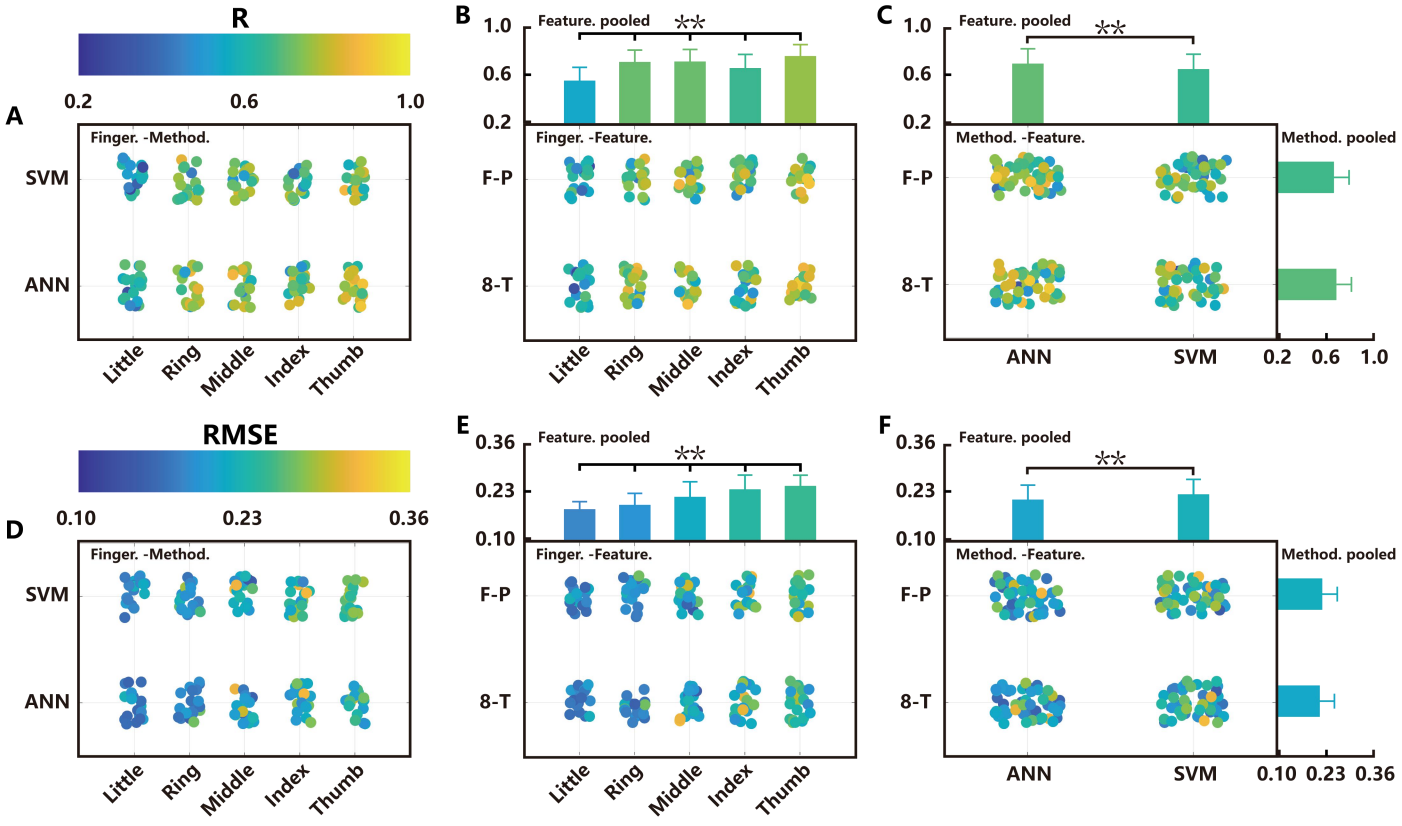

Fig. S8. The effects of features and learning methods for fingers energy. In order to assess which combination of features and learning methods could apply to the energy-based interface, a ten-fold cross-validation procedure was used to evaluate the overall statistical performance of both different features (E-T and F-P) and learning methods (ANN and SVM). We showed the result from the three-way analysis of variance (features, methods, and fingers) in the total variation (R; A, B, and C) and the total residual error (RMSE; E, F, and G). Each small colored dots represent one test of energy estimation. **P< 0.01. Data show means ± SD.

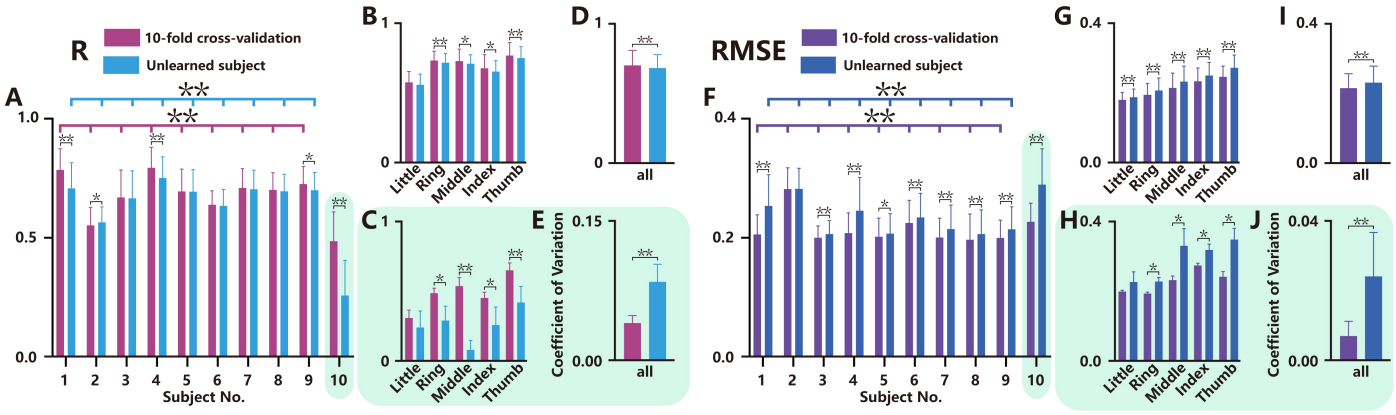

Fig. S9. The generalization of across subjects. To assess the degree to whether the energy-based interface applies to unlearned subjects, we used another ten-fold cross-validation procedure whose testing datasets from one subject totally while training datasets from other subjects, relative to the previous test. **(A)** Total variation (R) across subjects. **(B)** Total variation for single fingers (subject 1-9). **(C)** Total variation for single fingers (subject 10). **(D)** Total variation across all fingers (subject 1-9). **(E)** coefficient of variation of the total variation across all fingers (subject 10). **(F)** Total residual error (RMSE) across subjects. **(G)** Total residual error for single fingers (subject 1-9). **(H)** Total residual error for single fingers (subject 10). **(I)** Total residual error across all fingers (subject 1-9). **(J)** coefficient of variation of total residual error across all fingers (subject 10). *P< 0.05, **P< 0.01. Data show means ± SD.

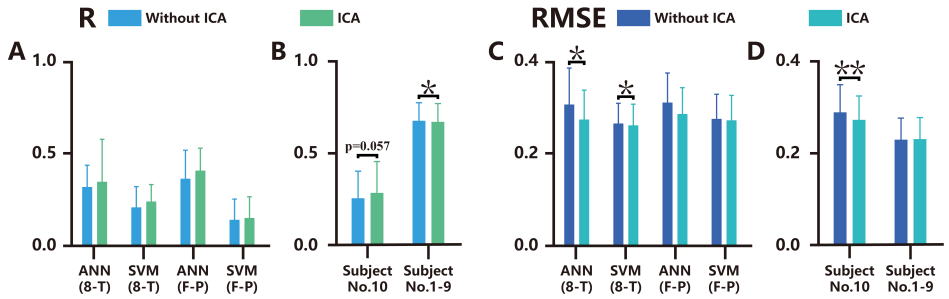

Fig. S10. Comparison of the models with ICA or without. To further assess whether the ICA model trained with the standard data applies to the subject contaminated with noise, we rebuilt a model using the synergy matrix decomposed by standard data from subject 1-9. Also, the model evaluation was accomplished through 10-fold cross-validation whose datasets divided by subjects. **(A)** Total variation (R) across conditions. **(B)** Total variation across all conditions. **(C)** Total residual error (RMSE) across conditions. **(D)** Total residual error across all conditions. *P< 0.05, **P< 0.01. Data show means ± SD.

Table 1. Experiment 1: the expression of unlearned continuous hand motions. To test the expression of multiple hand motions based on fundamental energy mode, we had the participant repeatedly sequential perform these randomly selected hand motions as faster as possible (repeated 5 times under each condition).

Hand	ICA	Subject \Completion time (s)					
		S5	S6	S7	S8	S9	S10
Trained hand (left hand)	Without ICA	90.40	80.62	90.70	85.82	96.69	102.78
		79.57	73.56	91.63	72.34	88.63	82.87
		80.76	78.10	75.67	67.52	69.45	78.17
		81.55	67.80	88.61	61.26	81.92	81.16
		75.30	63.65	82.37	66.52	66.30	69.58
	With ICA	93.27	81.14	83.44	76.02	89.81	82.25
		88.78	66.35	82.99	74.71	96.77	78.25
		76.30	72.91	91.52	73.98	88.86	77.65
		81.90	63.67	68.26	81.96	87.72	81.11
		73.22	71.30	82.30	67.32	72.13	70.24
Untrained hand (right hand)	Without ICA	89.90	89.66	87.80	66.87	88.96	411.61
		81.47	81.39	79.94	89.19	100.86	-
		80.90	75.55	102.27	77.94	79.76	-
		76.72	67.00	67.94	72.31	71.19	-
		71.84	71.41	102.27	59.76	69.64	-
	With ICA	85.48	88.34	71.99	79.30	103.04	84.79
		90.77	76.02	83.19	93.24	85.67	80.35
		79.66	72.34	83.60	79.25	76.95	82.82
		84.13	67.52	94.13	81.48	83.94	63.60
		76.23	62.26	87.20	73.90	89.26	67.07

Table 2. Experiment 2: the amount of single finger energy. To test the degree to the energy-based interface controls the amount of finger energy, we had the participant repeatedly perform these selected hand motions by controlling a bionic hand whose fingertips were fitted with steel needles while ensuring breaking/non-breaking the balloon (repeated 10 times under each condition; subject 5-9).

Hand	Balloon	Finger	Subject \Success times				
			S5	S6	S7	S8	S9
Trained hand (left hand)	Non-break	Index finger	7	8	9	9	10
		Middle finger	8	7	8	6	7
		Ring finger	9	10	7	10	8
		Middle-ring finger	9	9	8	9	7
		Index-middle finger	8	10	9	8	8
	Break	Index finger	6	8	9	7	6
		Middle finger	6	7	8	7	8
		Ring finger	8	7	6	8	5
		Middle-ring finger	8	8	8	8	7
		Index-middle finger	7	8	9	9	9
Untrained hand (right hand)	Non-break	Index finger	6	8	10	9	7
		Middle finger	7	8	9	7	9
		Ring finger	7	10	9	8	7
		Middle-ring finger	7	10	9	9	8
		Index-middle finger	7	9	8	7	10
	Break	Index finger	6	7	8	8	7
		Middle finger	7	6	7	7	7
		Ring finger	7	8	6	6	6
		Middle-ring finger	8	7	8	8	6
		Index-middle finger	9	8	8	7	7

Table 3. Experiment 3: the control of single finger energy in real-time. To assess the degree to control the finger energy in real-time, we had the participant repeatedly punch a hole in the plasticine (~1mm thickness) attached to the fixed balloon by using single fingers, while not breaking the balloon (repeated 10 times under each condition; subject 5-9).

Hand	Finger	Subject \Success times				
		S5	S6	S7	S8	S9
Trained hand (left hand)	Index finger	10	10	9	10	10
	Middle finger	10	10	10	9	10
	Ring finger	10	9	10	10	10
Untrained hand (right hand)	Index finger	10	10	10	10	10
	Middle finger	9	10	9	10	10
	Ring finger	10	10	10	10	8

A novel energy-motion model for continuous sEMG decoding: from muscle energy to motor pattern

Gang Liu, Lu Wang, and Jing Wang

***Abstract*—Myoelectric prosthetic hands create the possibility for amputees to control their prosthetics like native hands. However, user acceptance of the extant myoelectric prostheses is low. Unnatural control, lack of sufficient feedback, and insufficient functionality are cited as primary reasons. Recently, although many multiple degrees-of-freedom (DOF) prosthetic hands and tactile-sensitive electronic skins have been developed, no non-invasive myoelectric interfaces can decode both forces and motions for five-fingers independently and simultaneously. This paper proposes a myoelectric interface based on energy allocation and fictitious forces hypothesis by mimicking the natural neuromuscular system. The energy-based interface uses a kind of continuous "energy mode " in the level of the entire hand. According to tasks itself, each energy mode can adaptively and simultaneously implement multiple hand motions and exerting continuous forces for a single finger. Also, a few learned energy modes could extend to the unlearned energy mode, highlighting the extensibility of this interface. We evaluate the proposed system through off-line analysis and operational experiments performed on the expression of the unlearned hand motions, the amount of finger energy, and real-time control. With active exploration, the participant was proficient at exerting just enough energy to five fingers on "fragile" or "heavy" objects independently, proportionally, and simultaneously in real-time. The main contribution of this paper is proposing the bionic energy-motion model of hand: decoding a few muscle-energy modes of the human hand (only ten modes in this paper) map massive tasks of bionic hand.**

***Index Terms*—Myoelectric interface, amputees, prosthetic hand, electromyogram, real-time systems, conservation of energy.**

I. Introduction

HAND loss is a highly disabling event, and markedly affects the quality of life [1]. In order to replace the capabilities lost, the replacement should be designed to faithfully mimic the native hands, providing the user with intuitive control, sufficient feedback, and multiple functions (Fig. 1) [1-4]. Sixty years ago, the advent of a myoelectric prosthetic hand, an externally powered prosthesis extracting motion intent from electromyogram (EMG) signals, brought a promising approach [5]. Up to now, prosthetic hands and myoelectric interfaces have been investigated extensively. Nevertheless, these advances did not proceed at the same speed. Recently, advances in mechatronics have yielded tactile-sensitive skins [6], bionic sensory feedback [1, 7], and multi-fingered prosthetic hands capable of mimicking the functions that the biological hand provides [8]. However, to our knowledge, no non-invasive myoelectric interface achieves the recognition of both multiple motions and forces of a single finger, matching state of the art in multi-DOFs prosthetic hands and tactile feedback.

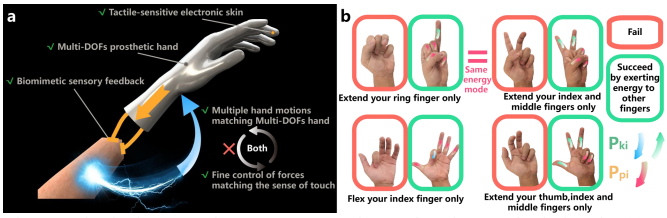

Fig. 1. Bionic frame and current status of myoelectric prosthetic hands. (a) A closed-loop myoelectric prosthetic hand can be divided into three parts: user intent, control, and sensory feedback. The green " √ " symbol indicates the technology has been developed, and the red " × " symbol indicates the technology is still unclear. The ideal hand requires excellent control of single fingers. First of all, performed with a certain task such as turning a door handle or grabbing a car key, the amputees must be able to enforce the correct grasping motions. Second, the amount of force involved in the grasp must be controlled so that it is possible to grab, e.g., both a hammer without letting it slip and an egg without breaking it. Third, feedback to the patient is paramount. (b) Example of the primary mechanism of human hand mimicked in the present study (more examples in Supplementary Materials). We sought to regard the whole manual task as energy transfer, mimicking the adaptive mechanism of the human hand. The direction of arrows indicates "the direction of energy", and the same direction for five energies means that these hand motions could be achieved by the same energy mode. P_{ki} expresses the kinetic energy of the i -th finger, while P_{pi} expresses the potential energy of the i -th finger.

The earliest versions of the myoelectric interface are dated to the 1950s and 1960s [9]. The interface usually takes an on/off approach. Two bipolar EMG electrodes are placed at the flexors and extensors of the residual limb to record information about the neuromuscular activity. For each processing interval, the EMG amplitude is compared with a predefined threshold. When the threshold is exceeded, the corresponding function (e.g., hand close) is actuated at a speed fixed or proportional to

Manuscript received XXX; revised XXX; accepted XXX. date of publication XXX; date of current version XXX. This work was supported by the Science and Technology Project of Shaanxi Province (2019SF-109). (Corresponding author: Jing Wang)

Gang Liu, Lu Wang and Jing Wang are with Institute of Robotics and Intelligent Systems, School of Mechanical Engineering, Xi'an Jiao Tong University, Xi'an 710049 China (e-mail: lg_7777777@stu.xjtu.edu.cn; iamwanglu@stu.xjtu.edu.cn; e-mail: wangpele@gmail.com).

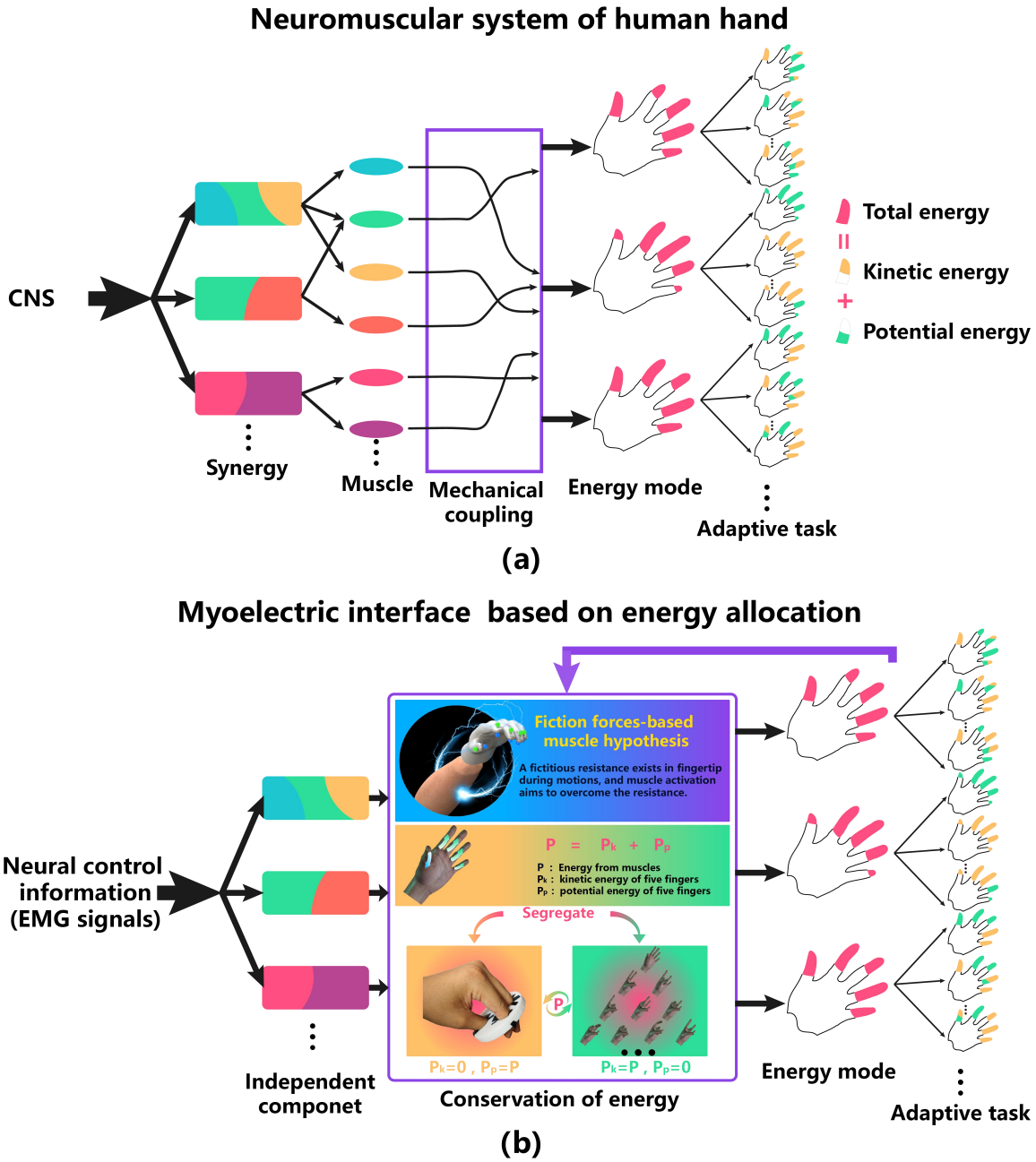

Fig. 2. Scheme for the biomimetic myoelectric interface. (a) Schematic diagram of the neuromuscular system of human hand, including muscle synergy, mechanical coupling, and the conversion of kinetic energy and potential energy adaptively. (b) Schematic diagram of the proposed myoelectric interface. The energy of muscles is transferred through mechanical coupling to five-fingers, which performs manual tasks by the conversion of kinetic energy and potential energy adaptively. The essence of the myoelectric interface is the total energy allocation of five-fingers. Furthermore, the size of colored area on single finger expresses the amount of energy.

the EMG amplitude. This approach can provide intuitive control of smooth movements so that it is still used by the vast majority of commercial prostheses today. For example, MyoBock, the most popular myoelectric prosthetic hand in the world, enables control of hand close and open [8]. Besides, to control another DOF like the rotation of the wrist, the user can switch the active DOF by a co-contraction of both muscle groups or other heuristics [10]. While intuitive, this interface is limited to control only one DOF at the same time and provides little dexterity.

In order to control more DOFs, intensive research has focused on motion classification that assigns EMG features to a discrete set of motions [11-13]. Tremendous success has been achieved in this line of research. With properly designed feature extraction and classifier, it is possible to achieve extremely high classification accuracies (90–95%) on a large repertoire of motions (21 classes) [12]. Moreover, Akira et al. have demonstrated that a mechanism classifying unlearned combined motions from a dataset of learned single motions [13]. In principle, it can be extended to the classification of any hand motions. Despite its success in research, classification in its basic form only allows for the sequential activation of motions, precluding intuitive control of smooth movements. An error may lead to a completely unwanted motion that may

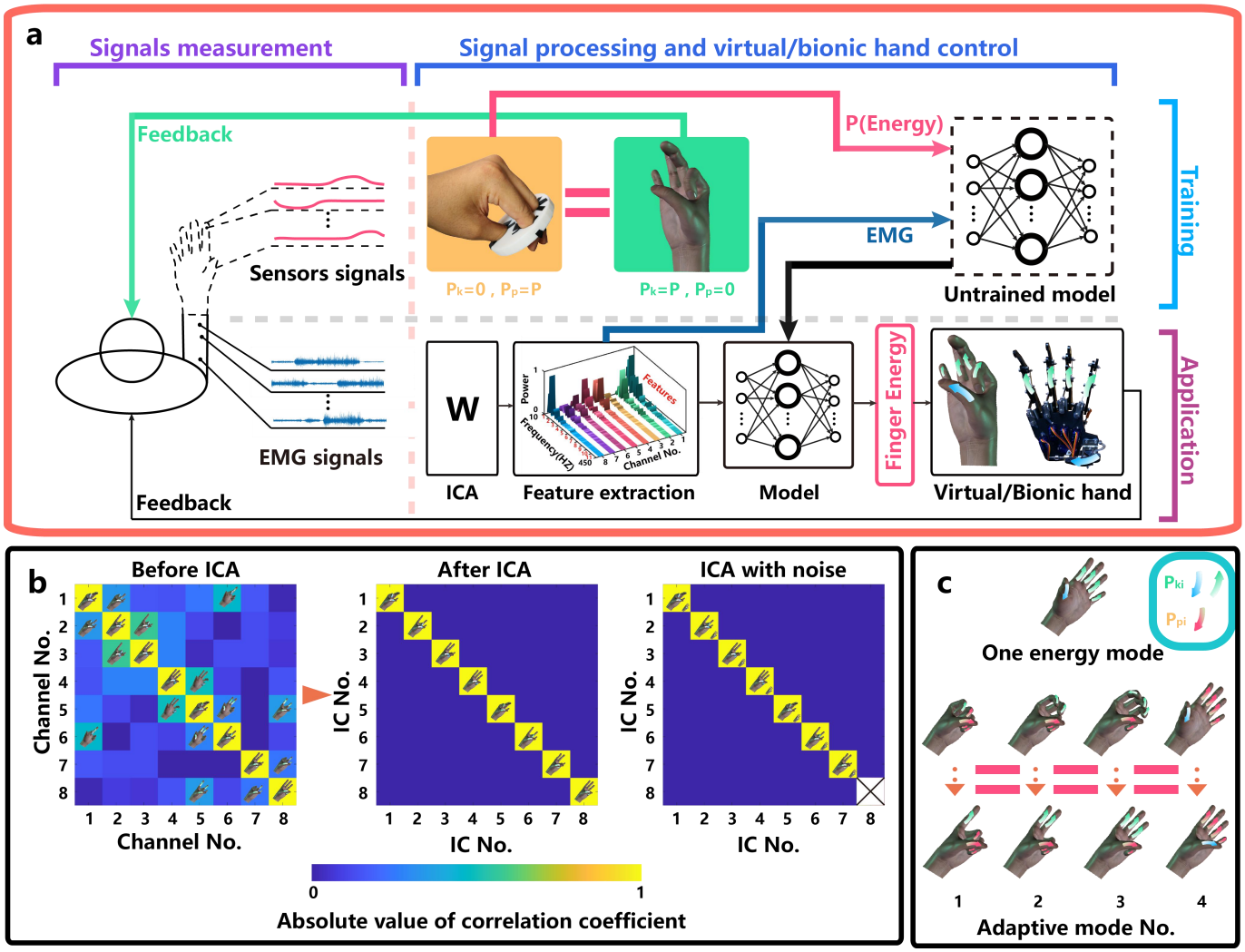

Fig. 3. Overview of the myoelectric interface based on the conservation of energy. The myoelectric interface (a) is composed of training and application stages. Both stages consist of signals measurement and signal processing and virtual/bionic hand control. Note that, in the training stage, the sensor signals can be measured on the intact side of the user. Besides, independent component analysis (ICA) decomposes a synergy matrix that represents muscle activation. The synergy matrix is used to extract muscle synergy and improve robustness (b). Furthermore, each energy mode can extend many other hand tasks adaptively (c). P_{ki} expresses the kinetic energy of the i -th finger, while P_{pi} expresses the potential energy of the i -th finger.

compromise the full task [3]. Therefore, the pattern recognition-based interface has not been widely utilized in commercial prostheses.

Recently, to overcome the limitations of the classification-based approaches, regression-based approaches have been proposed. They attempt to estimate a proportional activation for each DOF. Most research has focused on the estimation of kinematic joint angles of the wrist [14-16]. However, this approach may not achieve to manipulate small objects due to the missing force information. Katie et al. succeed in filling this missing information with 'shared control' (that is, automation of some portion of the motor command to achieve grip force) [17]. However, it may lead to unintuitive and unnatural feedback for the user. For this issue, Jiang et al. have proposed a nonnegative matrix factorization (NMF) approach based on the concept of muscle synergy [18]. This approach can extract the neural control information from the surface EMG, and generate force outputs of the wrist. Although the results presented are promising, the estimation of forces and kinematics of each finger has rarely been investigated.

The sophisticated hand control is a peculiar characteristic of higher primates [19]. The continuous decode of five-fingers requires more massive training datasets (machine learning method) or more complicated priori conditions [18]. More importantly, unlike the wrist, both mechanical coupling and neuromuscular control limit to finger independence [20, 21]. For instance, active movement at one finger may result in some movement at another finger. Previous approaches estimated a proportional activation for each DOF might not apply to five-fingers [21]. Recordings of finger movements during grasping, typing, or piano playing reveal that humans rarely move one finger alone but multiple fingers simultaneously. The degree of simultaneous motion depends on the behavioral task performed [21]. Conservation of energy — regard the whole manual task as an energy transfer—is likely to provide a new strategy [22].

Here, this paper proposes a myoelectric interface based on

the conservation of energy (Fig. 2 and Fig. 3). The forearm muscle controls fingers, which is essentially a transmission of energy from forearm muscles to five-fingers. Using conservation of energy rather than dynamics or kinematics methods eliminates complex transfer processes (e.g., mechanical coupling) and allows exploring the energy allocation of five-fingers (called "energy mode"). One continuous energy mode can adaptively extend to multiple motions or forces according to the task itself (e.g., mechanical coupling of the task and physiological coupling of five-fingers [20, 21]) ; also, some unlearned energy modes can be expressed by a few learned energy modes (Fig.3c and fig.4e).

This paper consists of the proposed myoelectric interface, three sets of exploratory operational experiments, and off-line analysis. Section II introduces an overview of the bionic interface. Section III describes the details of the interface and experiments. Section IV shows the results of experiments and off-line analysis. In Section V, we discuss the results and limitations and draw the conclusion. Note that we provided Supplementary Materials and Movies, and "Fig. S" can be found in Supplementary Materials.

II. Bionic Inspiration and Interface Overview

Inspired by the neuromuscular system of human hand, we propose a myoelectric interface based on energy allocation. The scheme for the strategy is shown in Fig. 2. We imitate two stages that the central nervous system (CNS) activates muscles and that muscles control fingers to complete the task adaptively (Fig. 2a). For the first stage, strong evidence from EMG of frogs [23], cats [24], primates [25], and humans [26] has demonstrated the existence of muscle synergy in the neuromuscular system. Concretely, a group of synergetic muscles instead of one is activated to perform a certain task, which allows the CNS to achieve muscle activation by controlling a few synergies. For the second stage, the energy of muscles is transferred through mechanical coupling to five-fingers, which performs manual tasks by the conversion of kinetic energy and potential energy adaptively [19, 21].

In light of this, we modularize the model of the myoelectric interface (Fig. 2b). Firstly, control signals are obtained using the filtered EMG recordings as input to a synergy matrix that represents muscle activation strategies from the individual muscles to muscle groups, which highlight the information of synergies from CNS. Secondly, controlling fingers through the forearm muscles are regarded as an energy transfer process based on energy conservation. To unify the static force and motion condition, we assume that a fictitious resistance exists in fingertip during flexion and extension of each finger, and muscle activation aims to overcome the resistance. Thus, the total energy of a finger can be regarded as a sum of the kinetic and potential energy, consisted of three forms: kinetic energy, potential energy, or coexistence of kinetic energy and potential energy. Under a certain activation of muscles, the total energy for a single finger is constant, and there is only one pattern of the total energy allocation for five-fingers. The essence of the myoelectric interface is the total energy allocation of five-fingers. Therefore, we can solve this problem through two extreme conditions of energy transfer.

Figure 3 shows an overview of the proposed myoelectric interface. To simplify the model, we utilize the conditions of wholly transferred kinetic energy or potential energy. The five-fingers energy of the operator was estimated by the bionic model using independent component analysis (ICA) and conservation of energy, thereby allowing the expression of the unlearned hand tasks via a few learned energy modes adaptively [21, 27].

III. Materials and Methods

A. Scheme for the bionic myoelectric interface

From the perspective of information and energy transfer, the neuromuscular system of humans hand consists of muscle synergy, mechanical coupling, and the adaptive conversion of kinetic energy and potential energy (Fig. 2 and fig. S1). Therefore, we mimic these parts to designed our model.

1) ICA to mimic muscle synergy

Evidence from a large number of animal experiments has been demonstrated that the CNS achieves muscle activation by controlling a small number of synergies rather than controlling individual muscles [23-25, 28, 29]. Briefly, muscle synergy pattern can be expressed by the activation of individual muscles $[m_1(t),m_2(t),\cdots,m_n(t)] \in \Re^n$ (n is the number of muscle)

$$u(t) = F^{trans}(m_1(t),m_2(t),\cdots,m_n(t)) \quad (1)$$

Where $u(t) = [u_1(t),u_2(t),\cdots,u_m(t)] \in \Re^m$ (m is the number of synergy patterns and $m \le n$) and $F^{trans}(\cdots)$ is a function that transforms the muscle activation into a smaller number of synergies. Previous experiments of frogs [28] and rats [29] demonstrated that we could use ICA to extract these muscle synergy patterns. Therefore, muscle synergy pattern $u(t)$ is extracted from the time-series EMG pattern $[s_1(t),s_2(t),\cdots,s_n(t)] \in \Re^c$ ($c$is the number of EMG electrodes and $c \ge m$)

$$u(t)+\mathrm{e}(t) = F^{ICAtrans}(s_1(t),s_2(t),\cdots,s_c(t)) \quad (2)$$

Where $F^{ICAtrans}(\cdots)$ is a function that transforms the time-series EMG pattern into a smaller number of synergies, and $e(t)$ is the noise of the system (Fig. 3b). $u(t)$ is regarded as the information from CNS.

2) Energy transfer applied to human hand

Both mechanical coupling and neuromuscular control limit to finger independence [20, 21]. For example, active movement at one finger may lead to some movement at another finger (Fig. S1). To implement the fluid decoding of a single finger, we, therefore, sought to regard the whole manual task as energy transfer, mimicking the adaptive mechanism of the human hand. Applying the conservation of energy to the humans hand can be expressed as the following formula (Fig. 2b).

$$P = P_K + P_P \quad (3)$$

$$\Delta P_K = -\Delta P_P \quad (4)$$

Where P is the energy from muscles to hand, P_K is the kinetic energy of hand, P_P is the potential energy of hand (usually existing in the form of strain energy), ΔP_K is the amount of change of kinetic energy, and ΔP_P is the amount of change of potential energy. Also, the energy transfer can be phrased as follows at the level of a single finger.

$$P = \sum_{f=1}^{5} P_f^s, \quad P_K = \sum_{f=1}^{5} P_{k,f}, \quad P_P = \sum_{f=1}^{5} P_{p,f} \tag{5}$$

$$\Delta P_P = \sum_{f=1}^{5} \Delta P_{p,f}, \quad \Delta P_K = \sum_{f=1}^{5} \Delta P_{k,f} \tag{6}$$

Where $\{P_1^s, P_2^s, \cdots, P_5^s\} \in \Re^5$, $\{P_{k,1}, P_{k,2}, \cdots, P_{k,5}\} \in \Re^5$ and $\{P_{p,1}, P_{p,2}, \cdots, P_{p,5}\} \in \Re^5$ are the total, kinetic, potential energy for each finger, respectively. $\{\Delta P_{k,1}, \Delta P_{k,2}, \cdots, \Delta P_{k,5}\} \in \Re^5$ and $\{\Delta P_{p,1}, \Delta P_{p,2}, \cdots, \Delta P_{p,5}\} \in \Re^5$ are the amount of change of kinetic, potential energy for each finger, respectively. In addition, each finger satisfies the following conditions.

$$P_f^s = P_{k,f} + P_{p,f}, \quad f \in \{1,2,3,4,5\} \tag{7}$$

Here, according to the adaptive mechanism of the fingers in task [20, 21] and muscle synergy [13], we assume that a fictitious resistance exists in fingertip during flexion and extension of each finger, and muscle activation aims to overcome the resistance, so as to unify the static force and motion condition. Thus, the energy transfer of the single finger is as follows.

$$\Delta P_{k,f} = -\Delta P_{p,f}, \quad f \in \{1,2,3,4,5\} \tag{8}$$

In other words, for a certain muscle activation, although the form of energy is uncertain, the total energy of the single finger is a constant. Therefore, this process recasts the decoding problem as the problem of energy allocation of the five-fingers (energy mode; the adaptive and expansive expression are shown in fig.3c).

To simplify the model, we utilize the conditions of wholly transferred kinetic energy P_K^{ext} or potential energy P_P^{ext}.

$$P_K^{ext} = P_P^{ext} = P \tag{9}$$

Also, the form of a single finger is as follows.

$$P_{k,f}^{ext} = P_{p,f}^{ext} = P_f^s, \quad f \in \{1,2,3,4,5\} \tag{10}$$

Where $P_{k,f}^{ext} \in \{P_{k,1}^{ext}, P_{k,2}^{ext}, \cdots, P_{k,5}^{ext}\} \in \Re^5$ and $P_{p,f}^{ext} \in \{P_{p,1}^{ext}, P_{p,2}^{ext}, \cdots, P_{p,5}^{ext}\} \in \Re^5$ are the wholly transferred kinetic energy or potential energy for a single finger. Furthermore, with the help of an additional system, according to the principle of virtual work, the wholly transferred potential energy should be equal to the amount of change of internal energy of the additional system (Fig. 2b and fig. 3a).

$$P_{p,f}^{ext} = W_{p,f}^{ext} = f_f^{ext} \cdot \delta_f^{ext}, \quad f \in \{1,2,3,4,5\} \tag{11}$$

Where $W_{p,f}^{ext}$ is the work of the energy transfer from finger to the additional system, f_f^{ext} is the force applied to the additional system, and δ_f^{ext} is the virtual displacement. Besides, comparing with (1), the energy of the five-fingers is expressed as the following formula.

$$P_f^s = P_{k,f}^{ext} = P_{p,f}^{ext} = f_f^{ext} \cdot \delta_f^{ext}, \quad f \in \{1,2,3,4,5\} \tag{12}$$

Then, we utilize the two extreme conditions of energy transfer simultaneously to solve the total energy for each finger, as shown in figure 3a.

B. Experimental protocol

We performed off-line analysis and three sets of operational experiments in which we decoded the finger energy of subjects using EMG signals recorded from their forearms. We recruited ten able-bodied subjects (subjects 1, 2, 3, …, 10) for the study (note that the EMG signals from subject 10 are contaminated with noise due to electrode shifts [30] and one lift-off electrode [31] intentionally in training stage).

1) Subjects and EMG recording

In this study, 10 able-bodied subjects (two females, eight males, aged 26.4±1.43 years) gave informed consent to participate in the experiment protocol. All participants were right-handed. We performed training stages in all experiments with their left hands for convenient operations. For the right hands, the electrodes were placed in the same positions as the left hand in operational experiments. Also, these subjects' hands are similar in size due to the forces capture device (Fig. 4).

According to anatomy and kinesiology of hand [32], we recorded the EMG activity from eight extrinsic muscles of the forearm of all subjects. As shown in figure S4, four flexor muscles and four extensor muscles related to hand or finger movements were selected.

2) Training stages

a. System setup

The system is mainly composed of a multichannel surface electromyography device, a finger force capture device, and a personal computer (Fig. 4). Surface EMG signals, as well as the continuous five-fingers forces in both finger flexion and extension directions with visual feedback of virtual hand, were recorded simultaneously. Among them, proportional five-fingers forces indicate the potential energy that converted into the internal energy of the capture device. Visual feedback of the virtual hand represents kinetic energy that is completely converted by potential energy for each finger (kinetic energy is in direct proportion to the square of the speed of virtual fingers). Additional information regarding the devices can be found in the Supplementary Materials and movies.

b. Data collection

The participants were individually seated in a comfortable chair in front of a table and were asked to place left hands on the table and watch the LCD monitor. The arm with EMG electrodes was supported by a spongy cushion, and the fingers

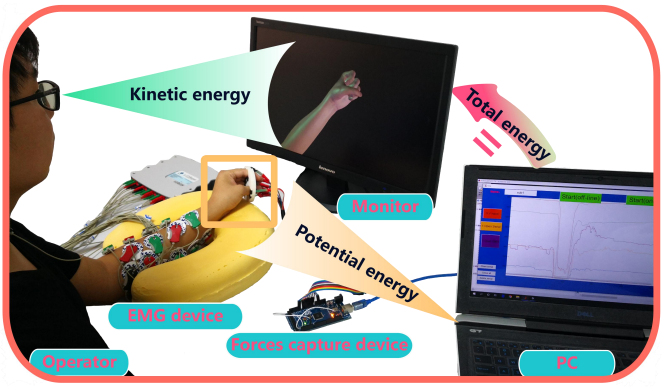

Fig. 4. Hardware structure for training states. Although the learning method we selected, such as ANN or SVM, is similar to previous researches that recorded motions or force of the wrist, the difference of our interface is that we had users perform tasks that represent energy modes in the level of the whole hand. It is very convenient to extend massive manual tasks by training a few energy modes about the entire hand, rather than a lot of motions or single-finger force.

were fixed in the fingertip force capture device. All subjects participated in the data collection and were included in off-line analyses. Besides, the EMG signals from subject 10 are contaminated with noise due to electrode shifts [30] and one lift-off electrode [31] intentionally. The subject was tasked with moving virtual fingers simultaneously to achieve the target gestures (Movie S6). The task consisted of the target movements of five-fingers, single-finger, two-fingers, and three-fingers flexion and extension simultaneously.

3) Online experiment stages

After training, some energy models using artificial neural network (ANN) learning method was obtained (see *Data analysis part*). We performed the following experiments using these models.

a. Experiment 1: the expression of unlearned continuous hand motions

Attribute	*Condition*
Prepared models	(1) Models with non-ICA (2) Models with ICA
hand	(1) Trained hand (2) Untrained hand
Drive system	Virtual hand

With the evolution of limb in humans, hands have developed into a highly sophisticated system used for manipulative activities—tool use, preparing, and eating food [19, 33]. Today, as a result of cultural pressure, the complexity of the human hand motions has increased tremendously. Some tasks require different hand motions, such as turning a door handle or grabbing a car key. Other tasks require a more differentiated role for each finger, such as sewing, clicking the keyboard, playing musical instruments.

Some myoelectric interface implements the classification of many hand motions depending on large training datasets of target motions, resulting in an increased burden on users [11, 34]. We, therefore, sought to implement the expression of multiple unlearned hand motions by our energy-based interface only using a few energy modes.

To assess the benefit, we asked participants to perform these hand tasks in figure 5e as faster as possible from figure 5e1 to figure 5e13, continuously rather than individually. We examined two outcome measures: completion rate and completion time. Trial failure was defined as the participant voluntarily gave up the trail, analogous to give up manual tasks that use the prosthetic hand in ADLs.

Six subjects (subject 5,6,7,8,9,10) participated in this experiment. For this experiment, a total of 4 different experimental conditions were examined (Table S1 and fig. 5). Tests under each condition were performed five times. We first test the trained hand and later test the untrained hand, and alternately test the algorithm with ICA and without for each hand. Additionally, for the trained hand test, we did not re-position the electrodes relative to the training phase, and for the untrained hand test, we re-positioned the electrodes. Also, for normalized EMG reducing individual differences, at the beginning of the experiment, we asked participants to flex and extend their hands and fingers to try maximum contractions for the muscles in the forearm.

b. Experiment 2: the amount of single finger energy

Attribute	*Condition*
Prepared models	Models with ICA
hand	(1) Trained hand (2) Untrained hand
Drive system	Bionic hand

When manipulating objects, our native hands are good at exerting just exactly enough fingertip force on it [35]. For example, while the object is light and "fragile", such as a grape, our hands manipulate a "gentle" enough pinch not to cause any damage; while the object is heavy and slippery, such as a hammer, our hands can exert just enough pressure on an object to avoid slipping free from a stable grasp [36].

Some tests of manual dexterity do few benefits from force sensitivity—no penalty is incurred for exerting too much force on an object, such as the Box and Blocks Test and Action Research Arm Test. However, many tasks in activities of daily living (ADLs) are highly dependent on force sensitivity. In our test, we, therefore, designed the experiment in which prick suspended balloon with a needle. The balloon is "fragile" and "break" if exerted finger energy too much, while the balloon is "suspended" and "slip away" if exerted finger energy too little.

To test whether the energy-based interface distinguishes the amount of finger energy, we had the participant repeatedly perform these selected hand motions by controlling a bionic hand whose fingertips were fitted with steel needles on the premise of ensuring breaking/non-breaking the balloon (Fig. 6e and Movie S4).

Five subjects (subject 5,6,7,8,9) participated in this experiment. For this experiment, a total of 4 different experimental conditions were examined (Table S2 and fig. 6). Tests under each condition were performed ten times. We first test the trained hand and later test the untrained hand, and alternately test the experiment with breaking or non-breaking the balloon. When the participant was asked to perform the selected hand motion without breaking the balloon, trial failure

was defined as "breaking" the balloon or not accomplishing the selected gesture. When the participant was asked to perform the selected hand motion with breaking the balloon, trial failure was defined as "non-breaking" the balloon or not accomplishing the selected gesture.

Additionally, the perimeter of the balloon is was about 66 cm, and the length of the hanging rope is about 7 cm. The experimental balloons were counterbalanced to reduce quality effects. Each balloon is filled with 36 grams of plasticine (Fig. S6).

c. Experiment 3: the control of single finger energy in real-time

Attribute	*Condition*
Prepared models	Models with ICA
hand	(1) Trained hand (2) Untrained hand
Drive system	Bionic hand

Our native hands were exquisitely proficient at flexing the finger a just enough position and perform manual tasks precisely—e.g., combing hair or applying lipstick, depending on controlling finger energy in real-time [19]. To display noticeable results when exerting too much energy, we developed a closed-loop task punching a hole in the plasticine (~1mm thickness) attached to the fixed balloon with steel needles (Fig. 7e and Movie S5). Concretely, we had the participant repeatedly punch a hole in the plasticine (~1mm thickness) attached to the fixed balloon by using the index, middle and ring fingers, while not breaking the balloon.

Five subjects (Subject 5,6,7,8,9) participated in this experiment. For this experiment, both hands and selected fingers were examined (Table S3 and fig. 7). Tests under each condition were performed ten times. Success failure was defined as "punching" a hole with the selected finger under the unbroken balloon in 30 seconds (Fig. 7e and movie S5).

C. Data analysis

The formal scheme for the analysis of the EMG signals for the model: preprocessing steps, feature extraction, and the learning of models for EMG features and five-fingers energy features.

1) Data processing

This preprocessing step included two further preprocessing steps. During EMG recording, 16-channel EMG data has been band-pass filtered from 10 Hz to 450 Hz and notch filtered of 50 Hz to remove movement artifacts, high-frequency noise, and power line noise and its harmonics [37]. Firstly, by considering the clinical relevance of using single-differential EMG, the EMG data of 16-channels were further processed to produce 8 bipolar channels by subtracting each pair of adjacent channels along the muscle fibers as they are more tolerant of noise than monopolar ones [38]. Additionally, after the first step, ICA can be selected. In order to reduce the output variable dimensions, the finger power of one finger was calculated as the pressure of finger pulp minus the pressure of the finger dorsum. Finally, the power data of 10-channels were processed to 5-channels wherein the signs of the power represented the flexure and extension of fingers, and the absolute values of the power represented the magnitude of power. Secondly, a 200 ms sliding window with a 50 ms overlap was used to down-sampled to 6.67 Hz due to the difference in the sampling frequency between the EMG data and power data. The EMG data in the sliding window were prepared for feature extraction. The power data was filtered using a moving average window to improve movement smoothness towards online control. (more information in Supplementary Materials)

2) Feature extraction

The fundamental purpose of feature extraction is to emphasize the critical information in the recording signal while rejecting noise and irrelevant data. We chose two groups.

Over the past two decades, some EMG features have been widely used in research and clinical practice. In this study, six time-domain features and two frequency-domain features typically used for myoelectric interfaces [37, 38] were extracted from each EMG channel in the 200 ms sliding windows producing a set of 64 EMG features (8 features×8 channels). [E-T: Mean of absolute values, Variance, Waveform Length, Root-mean-square value, Willison Amplitude(WAMP), Zero crossing (ZC), Median Frequency(MDF), and Mean Frequency(MNF)]

Additionally, the EMG amplitude is a simple and useful feature, as evidenced by commercial prostheses [8]. To further improve the robustness to noise distinguishable by frequency band, we also extract the frequency-domain power (F-P) as features with a sample short-time Fourier transform, similar to amplitude in the different frequency band (Fig. S5), which produces a set of 88 EMG features (11 features×8 channels).

3) Learning methods

As two examples of learning methods, we explore two learning methods. Firstly, a multi-layer feedforward ANN was used to learn a mapping between the EMG signals and the five-fingers energy. The functional relationship predicted by the ANN can be written as:

$$P^{pre}(t) = NN(e(t),w) \tag{13}$$

Where $P^{pre}(t) \in \Re^{5\times1}$ are the predicted five-fingers power, $e(t) \in \Re^{64\times1}$ (E-T) or $e(t) \in \Re^{88\times1}$ (F-P) represent the EMG features, w are the weight parameters which represent the links between the nodes or neurons. The network is made up of an input layer, a hidden layer with a tanh activation function (the number of neurons: 10), and a single linear output layer. The training algorithm was Levenberg–Marquardt back-propagation. Secondly, the excellent performance of the support vector machine (SVM) applied to regression problems is known. SVM regression is statistical learning machines [39] that build an approximated map between samples drawn from an input space (under the standard i.i.d. sampling hypothesis) and a set of real value. As is standard, we use the radial basis function for regression.

4) Operational experiments

For all operational experiments, as an example, we used a 200 ms sliding window to extract F-P features and the ANN learning method to predict the energy of five-fingers online, and the online instruction update rate was kept at 200 Hz (5ms interval).

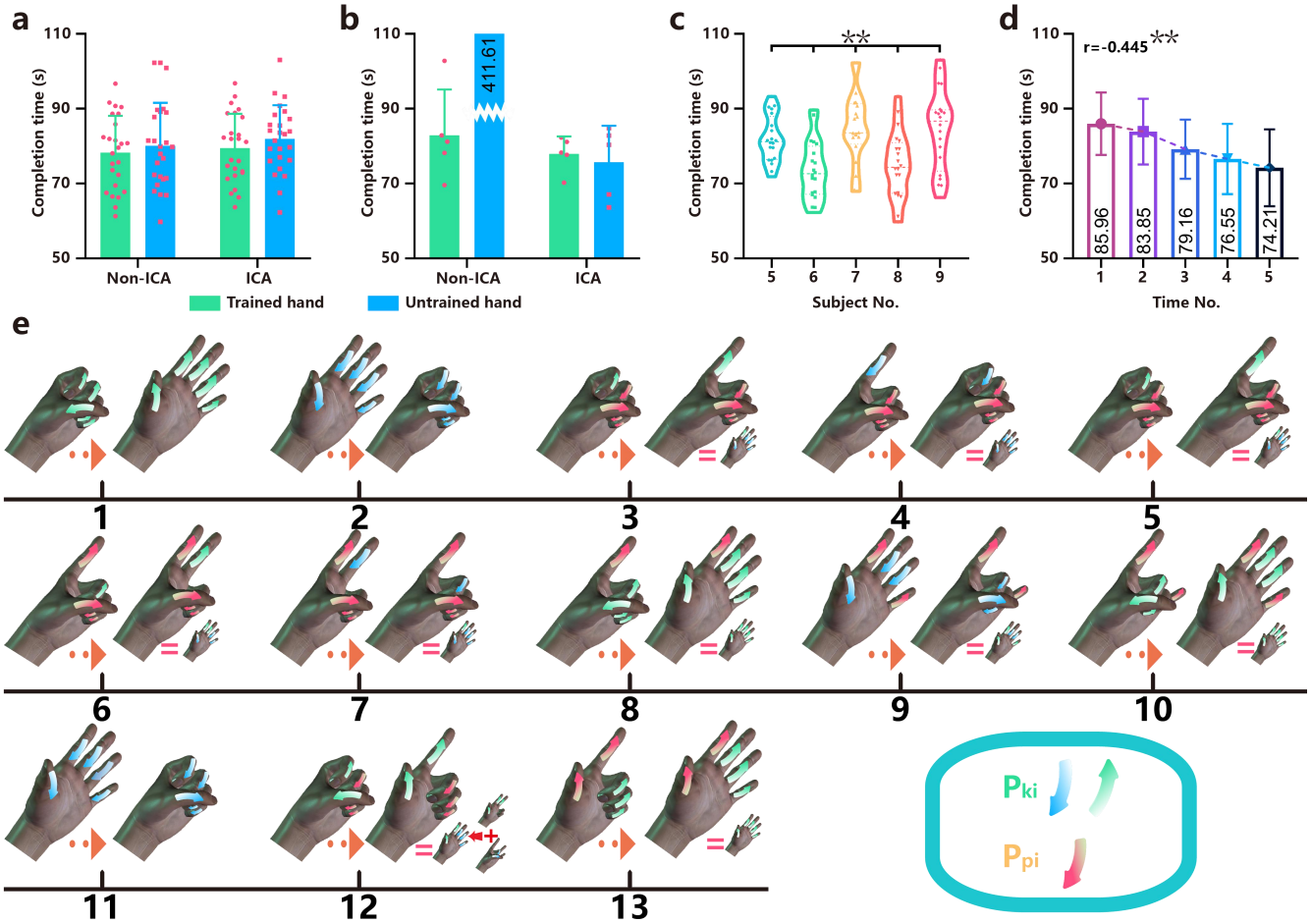

Fig. 5. Energy-based interface implements the expression of unlearned hand motions. To test the expression of multiple hand motions based on fundamental energy mode, we had the participant repeatedly sequential perform these selected hand motions as faster as possible (repeated 5 times under each condition). (a) The completion result of normal participants (subject 5-9). (b) The completion result of the participants whose EEG signals were contaminated with noise in training stage (subject 10). (c) Differences among participants in completion time (subject 5-9). (d) Faster with the number of operations. (e) Selected hand motions based or fundamental energy mode. [Note that, one continuous energy mode can adaptively extend to unlearned multiple motions or forces according to the task itself (e.g. mechanical coupling of task and physiological coupling of five-fingers)—e.g., the same energy model of e3 and e7; The unlearned energy mode can be expressed by fundamental energy mode—e.g., e12](In terms of motions, unlearned motions includes e3, e4, e5, e6, e7, e12, and e13). P_{ki} expresses the kinetic energy of the i -th finger, while P_{pi} expresses the potential energy of the i -th finger. *P< 0.05, **P< 0.01. Data show means ± SD.

IV. Result

A. Experiment 1: energy-based interface achieves the expression of unlearned continuous hand motions

All normal participants completed tasks successfully (100 of 100 times from subject 5-9; binomial test, $P < 0.0001$; Fig. 5a and Movie S1-3).

The energy-based interface requires the sensor signals from one hand, such as in the case of unilateral amputees, in training stages [40]. To test the performance of the proposed interface in the untrained hand, we had the participant respectively perform the above tasks with the trained hand or the untrained hand. As might be expected, given the similarity of both hands of one man in neuromuscular patterns, participants implement these motions not slower with the untrained hand than the trained hand through either ICA (81.96±8.95 s versus 79.47±9.15 s; paired t test, $P = 0.210$; Fig. 4a) or non-ICA algorithms (80.10±11.48 s versus 78.27±9.80 s; paired t test, $P = 0.435$; Fig. 5a). However, there were significant differences among participants (one-way ANOVA test, P <0.01; Fig. 5c), and it becomes significantly faster with the number of operations (correlation analysis, r=-0.445, P <0.01; Fig. 5d).

Additionally, the lack of robustness of myoelectric control approaches is one of the reasons for the limited transfer into clinical and commercial applications [41]. To test whether the bionic interface that includes the ICA matrix was resistant to the interference of noise, we had subject 10 respectively perform the above tasks with the algorithms of non-ICA or ICA. We found that subject 10 was able to perform these tasks with the untrained hand through ICA algorithms (5 of 5 times; binomial test, $P < 0.0001$; Fig. 5b), and as faster as with the trained hand (75.73±9.69 s versus 77.90±4.69 s; paired t test, $P = 0.621$; Fig. 5b). However, subject 10 might fail to achieve these tasks with the untrained hand through non-ICA algorithms (success times:1 of 5 times; binomial test, P =0.375; Fig. 5b). The ICA that mimics the muscle synergy of the neuromuscular system in the training stage increased the robustness of the myoelectric interface [Although participants implement these motions not significantly faster with ICA than without (untrained hand:81.86±8.95 s versus 80.10±11.48 s;

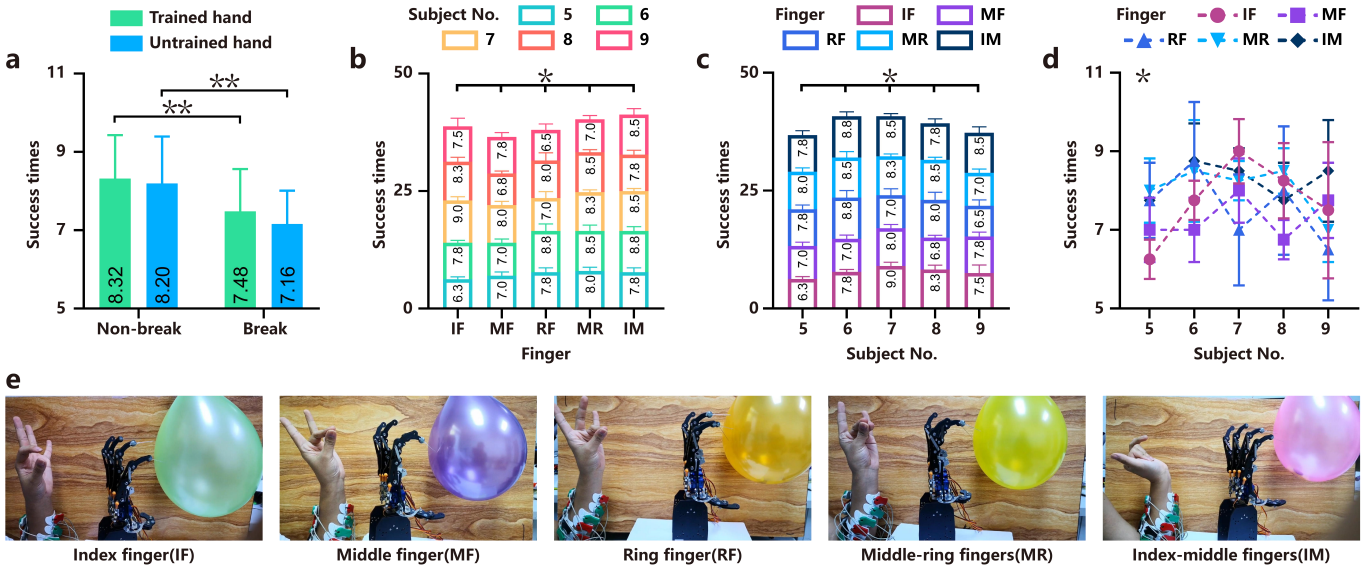

Fig. 6. Energy-based interface controls the amount of finger energy on the tasks pricking suspended balloons with a steel needle. To test whether the energy-basec interface distinguishes the amount of finger energy, we had the participant repeatedly perform these selected hand motions by controlling a bionic hand whose fingertips were fitted with steel needles, while ensuring breaking/non-breaking the balloon (repeated 10 times under each condition; subject 5-9). (a) Participants could exert just enough finger energy on a balloon. (b) Differences among fingers. (c) Differences among subjects. (d) Interaction effect between subjects and fingers. (E) Selected hand tasks according to ADLs. *P< 0.05, **P< 0.01. Data show means ± SD.

paired t test, $P = 0.429$; Fig. 5a)].

B. Experiment 2: energy-based interface controls the amount of single finger energy

The participant was able to exert just enough finger energy significantly better than chance (breaking: 366 of 500 trials; binomial test, $P < 0.0001$; non-breaking: 413 of 500 trials; binomial test, $P < 0.0001$; Fig. 6a). Besides, there was no significant difference between untrained hand and trained hand in the control of the amount of finger energy (non-breaking: 8.20 ± 1.19 times versus 8.32 ± 1.11 times; paired t test, P =0.671; breaking: 7.16 ± 0.85 times versus 7.48 ± 1.08 times; paired t test, P =0.148; Fig. 6a).

Contrary to expectation, it seemed not easy to prick suspended balloons with a needle relative to non-breaking counterpart (trained hand: 7.48 ± 1.08 times versus 8.32 ± 1.11 times; paired t test, P <0.01; untrained hand: 7.16 ± 0.85 times versus 8.20 ± 1.19 times; paired t test, P <0.01; Fig. 6a). One possibility, then, was the effect of balloons themselves. Thus, we explored the property of finger energy sensitivity by incorporated these two trails for reducing or eliminating potential confound. We found that there might be significant differences across fingers and subjects at the control of the amount of finger energy (Two-way ANOVA test, fingers: P <0.05; Fig. 6b; subjects: P <0.05; Fig. 6c), and different subjects might be adept in different fingers (Two-way ANOVA test, P <0.05; Fig. 6d).

C. Experiment 3: energy-based interface controls single finger energy in real-time

The participant punched a hole without breaking balloon at over 95% success rate (97.67 ± 5.04 % versus 95 %; one-sample t test, P =0.148; Fig. 7a). Furthermore, success rates with untrained hand and trained hand were at the same level in real-time, no matter which fingers were used (index finger: 100 ± 0.00 % versus 98 ± 4.47 %; paired t test, P =0.374; middle finger: 96 ± 5.48 % versus 98 ± 4.47 %; paired t test, P =0.621; ring finger: 96 ± 8.94 % versus 98 ± 4.47 %; paired t test, P =0.704; Fig. 7a).

D. Off-line analysis

In the studies described above, the energy-based interface has been shown to confer functional benefits through three sets of operational experiments. Our purpose for this analysis was to explore the characteristics of the energy-based interface further and explain why the interface shows great functional benefits. Two performance indices were chosen to evaluate the accuracy of the estimation in each finger energy. Pearson's correlation coefficient (R) was calculated to assess the total variation between the estimated and actual energy, while the root-mean-square error (RMSE) to describe the total residual error.

1) Energy-based interface achieves a continuous estimation of finger energy in real-time

Even an element of EMG datasets exists massive properties, the properties that similar in the group but different among groups should be selected as features for a better model, and learning methods should be adopted to distinguish these groups through features as far as possible. To the extent, the fitting model is the classification model whose classes is infinite and continuous.

To assess which combination of features and learning methods could apply to the energy-based interface, a ten-fold cross-validation procedure was used to evaluate the overall statistical performance of both different features (E-T and F-P) and learning methods (ANN and SVM). Figure 8 shows the continuous estimation results from 10 subjects for 10 test trials. The signs of value represent the flexion or extension of fingers,

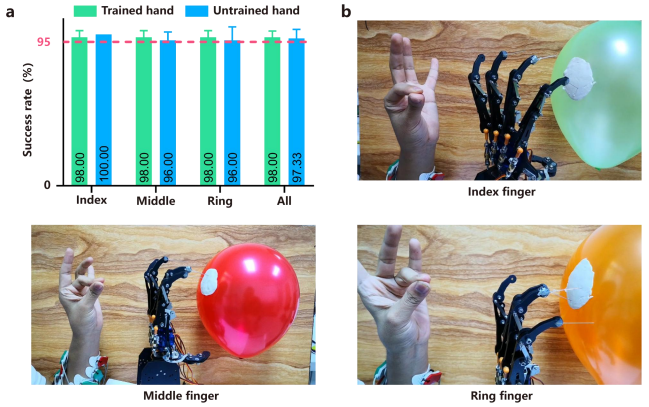

Fig. 7. Energy-based interface controls the single finger energy in real-time on the tasks punching a hole with a steel needle. To assess the degree to control the finger energy in real-time, we had the participant repeatedly punch a hole in the plasticine (~1mm thickness) attached to the fixed balloon by using single fingers, while not breaking the balloon (repeated 10 times under each condition; subject 5-9). (a) Participants could flex the finger a just enough position to punch a hole on the plasticine. (b) Example of tasks for the index, middle and ring fingers. Data show means ± SD.

and the absolute values represent the amount of finger energy. As an example, the equivalent state of kinetic energy and potential energy are shown from the data of subject 4. Figure S7 shows the confusion matrix for the estimation of the finger energy of subject 4. Although the confusion matrix shows some deviations, the user can correct the deviations in real-time, similar to the native hand [42, 43]. Furthermore, we found ANN outperformed SVM, whether in the total variation (0.699±0.124 versus 0.653±0.125; Three-way ANOVA test, P <0.01; Fig. S8C) or the total residual error (0.209±0.040 versus 0.223 ± 0.041; Three-way ANOVA test, P <0.01; Fig. S8F). Also, there are significant differences across fingers (R: Three-way ANOVA test, P <0.01; Fig. S8B. RMSE: Three-way ANOVA test, P <0.01; Fig. S8E). The lowly individuated fingers (ring and middle fingers) are likely performances better in the total variation [21].

Another way to assess the trait of the energy-based interface relative to classification-based is to characterize the accuracy of the estimation in a certain range of the amount of energy [13]. To test this extraordinary capability for single finger energy, we divided the amount of energy from zero to maximum voluntary energy (MVE) into 5 ranges (normalized energy; Fig. 9a and fig. 9c). The among ranges difference was significant, whether in the total variation (One-way ANOVA test, P <0.01; Fig. 9a) or the total residual error [One-way ANOVA test, P <0.01(logarithm of RMSE); Fig. 9a]. Also, the total residual error increase with the improvement in energy (correlation analysis, r=0.961, P <0.01; Fig. 9a), similar to the native hand [42, 43]. More interestingly, the distribution of relative energy (ratio of voluntary energy to MVE for the finger) is likely consistent with the usage frequency of the finger (Fig.9c). For instance, unconsciously exerting higher relative energy in the finger might signify more frequent use in ADLs. Furthermore, the model estimates the finger energy better for finger flexion than finger extension in total variation (the whole estimated energy relative to the whole actual energy rather than the statistics according to ten tests , 0.622 ± 0.034 versus

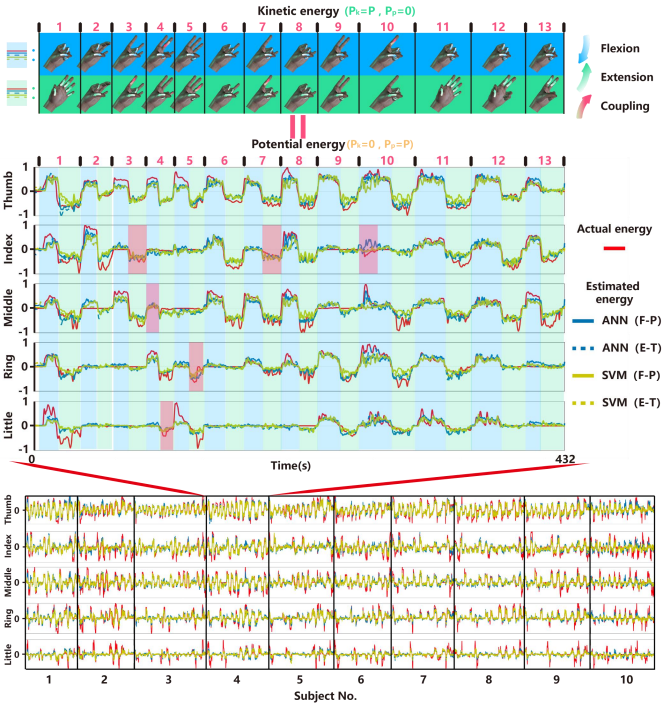

Fig. 8. Test data for ten subjects. Normalized five-fingers energy is shown in red solid lines, while the estimated results of the ANN and SVM method are shown in blue and green, respectively. The estimated energy of F-P features is shown in solid lines, and the energy of E-T features are shown in dotted lines. The signs of value represent the flexure or extension of fingers, and the absolute values represent the amount of finger energy. The data for subject 4, as an example, show the equivalent state of kinetic energy and potential energy. Besides, the blue arrows and shade bars represents the flexure of fingers, the green arrows and shade bars represents the extension of fingers, while the pink arrows and shade bars represent the coupled motion of fingers. P expresses the total energy of fingers, P_k expresses the kinetic energy of fingers, and P_p expresses the potential energy of fingers. Note that although some fingers remain stationary by overcoming the coupling, their muscle-energy modes are the same as in some hand motion.

0.495 ± 0.041; paired t test, P <0.01; Fig. 9b), presumably reflecting better performances in grabbing and pinching.

2) The generalization of across subjects is explored

Previous studies of muscle synergy for wrist demonstrated that humans have a similar anatomical structure and synergy [44, 45]. To assess the degree to whether the energy-based interface applies to unlearned subjects, we used another ten-fold cross-validation procedure whose testing datasets from one subject totally while training datasets from other subjects, relative to the previous test. Firstly, we found there are significant differences among subjects, whether in unlearned subjects (One-way ANOVA test, R:P <0.01; Fig. S9A; RMSE: P <0.01; Fig. S9F) or "learned" subject of the previous procedure (One-way ANOVA test; R: P <0.01; Fig. S9A. RMSE: P <0.01; Fig. S9F). Secondly, the "learned" subject outperformed the unlearned subject (paired t test; R:0.697±0.008 versus 0.680±0.007, P <0.01; Fig. S9D. RMSE: 0.215±0.041 versus 0.230±0.047, P <0.01; Fig. S9I), which presumably reflecting personalized anatomical structure [44]. Furthermore, as expected, when the training datasets did not contain the data of the testing subject, performance degradation in the subject contaminated with noise is more noticeable (Fig. S9C and fig. S9H); we also observed a significant increase in the coefficient of variation (paired t test; R:0.044 ± 0.009

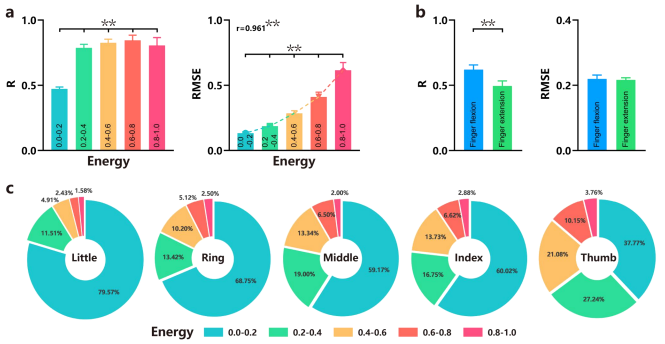

Fig. 9. The amount of five-fingers energy. To explore this extraordinary capability for a single finger in the amount of energy relative to the classification model, firstly, we divided the amount of energy from zero to maximum voluntary energy (MVE) into 5 ranges, and (a) explored the performance within each range; secondly, (c) we counted the distribution of these ranges for each finger, presumably consistent with the usage frequency of the finger in ADLs. Furthermore, for the performances in grabbing and pinching, (b) we also explored the accuracy according to the range of finger flexion and extension. **P< 0.01. Data show means ± SD.

versus 0.092±0.021, P <0.01; Fig. S9E. RMSE: 0.007±0.004 versus 0.024±0.013, P<0.01; Fig. S9J), highlighting the huge difference in performance across features and across learning methods for subject contaminated with noise.

3) ICA mimicking muscle synergy improves the robustness of the energy-based interface

In the studies described above, when trained with the subject contaminated with noise, the model shows performance better with ICA than without for standard data (Fig. 5b), presumably relying on information separation capacity of ICA (Fig.4b) [46]. Furthermore, ICA has been applied to extract synergies from the muscles of frogs [28] and rats [29]. To further assess whether the ICA model trained with the standard data applies to the subject contaminated with noise, we rebuilt a model using the synergy matrix decomposed by standard data from subject 1-9. Also, the model evaluation was accomplished through 10-fold cross-validation whose datasets divided by subjects. We found the model with ICA likely outperformed the previous model for the subject contaminated with noise (paired t test; R: 0.286 ± 0.148 versus 0.257 ± 0.171, P =0.057; RMSE: 0.274 ± 0.052 versus 0.290 ± 0.060, P <0.01; Fig. S10). However, the model with ICA showed no advantage in normal conditions (Fig. S10B and fig. S10D). Briefly, the major advantage of the ICA model lies in the capacity of reducing or eliminating the noise due to myoelectric prosthesis "aging" with time and use, such as failure electrodes and deformation, which increase the service life of the myoelectric prosthesis through recalibration (Fig.4b and fig. 5b).

V. Discussion and Conclusion

In the present study, we demonstrate that non-invasive myoelectric interfaces based on the conservation of energy — designed to mimic the natural neuromuscular system — can naturally decode both forces and motions for five-fingers, and confers to the user the ability to control five-fingers of bionic hand independently, proportionally, and simultaneously in real-time. Furthermore, the energy-based interface uses a kind of continuous "energy mode". One continuous energy mode can adaptively extend to multiple motions or forces according to the task itself (e.g., mechanical coupling of the task and physiological coupling of five-fingers [20, 21]), highlighting that the expression of multiple motions or forces requires only one energy mode, similar to the human hand [42, 43]. Also, the unlearned energy mode can be expressed by learned energy modes, highlighting the extensibility of this interface that learn small sample. Additionally, ICA mimicking muscle synergy improves the robustness, highlighting the capacity of reducing or eliminating the noise due to myoelectric prosthesis "aging" with time and use. This capacity increases the service life of the myoelectric prosthesis through recalibration. We evidence the above conclusions by three sets of operational experiments and off-line analysis.

The present results build on previous work, showing the prediction of unlearned combined motions using only learned single motions [13]. We extend these previous findings by showing that the expression of the unlearned energy mode by fundamental energy mode. Concretely, relative to previous work, the energy-based interface does not decide for a certain class, but instead, a continuous output value of energy is estimated for each finger. In this respect, our work is consistent with traditional proportional myoelectric control of the wrist or hand close and open [15, 41, 45, 47]. However, the estimation of forces and kinematics of single finger has rarely been investigated. Unlike the wrist, both mechanical coupling and neuromuscular control limit to finger independence [20, 21]. For instance, active movement at one finger may lead to some movement at another finger. Previous approaches that estimate a proportional activation for each DOF might apply to five-fingers. We extend these previous works to the estimation of energy of a single finger through two extreme conditions of energy transfer (Fig. 2). Furthermore, our method also derives the adaptive expression of multiple motions or forces according to the task itself — e.g., mechanical coupling of the task and physiological coupling of five-fingers [20, 21] (Fig. 1b, fig. 3c and fig. 5e). In the present study, we extend these previous works to a new technology based on the conservation of energy, an important interface benefiting from adaptive and continuous energy mode.

Amputees have expressed a desire for intuitive myoelectric control and the need for system robustness [48]. Ideally, when manipulating different objects in shape, weight, size, and fragile degree, they can voluntarily perform motions or exert forces at the single finger level in real-time (Fig. 1). Therefore, we sought to confers to the user this ability (Fig. 5, fig.6 and fig. 7). Furthermore, the adaptive property of the energy-based interface underlines the importance of the capacity of the user to interact with the machine and learn a new task in which the user is within the loop and can adapt to the control system. In the aspect of robustness, it also benefits from the adaptive property. Besides, a myoelectric signal comprises two states: a transient state emanating from a burst of fibers, as a muscle goes from rest to a voluntary contraction level, and a steady-state emanating during a constantly maintained contraction in a muscle [5]. The latter component dwarfs the former one in robustness [49], and the present system itself is

designed by energy transfer, which determines its used signal more steady. In addition, the present experiments explored ICA mimicking muscle synergy and demonstrated the capacity of reducing or eliminating the noise of failure electrodes and unstable connection via recalibration. Such capacity may prove more and more valuable with long-term use. With the advent of more and more prosthetic hands, this capacity may become an effective means of increasing the service life of commercial prostheses.

The main limitation of the current study is that no amputee was recruited. However, in previous studies, a large number of amputee subjects has been demonstrated similar to the non-disabled subjects in muscle activation [15, 45], and it is not likely that the motor learning ability of the amputees would be greatly affected by the limb deficiency. Besides, we also demonstrate that there no significant difference between the trained hand and untrained hand through operational experiments. It highlights the energy-based interface applies to the amputees (we, of course, exclude the amputee in muscular atrophy or non-existent measurable muscles). In fact, the present study emphasizes the excellent performance of the energy-based interface, and the user is not limited to the amputee, e. g., neurorehabilitation after stroke [50-52]. Besides, the energy-based interface ignores the amount of muscle activation to keep a certain angle, compared with others [14-17]. In general, it seems not important to realize a very accurate estimate of physical variables [47]. This simplification improves energy allocation much more stable and achieves the adaptive expression of multiple motions or forces. In comparison to the recent another study in finger angles [17], the energy-based interface does not predict the angles but rather to the transmission of energy from muscle to five-fingers (the amount of change of energy for a finger), which eliminate burden in muscle for maintaining posture or forces and retaining the benefit of instantaneous or short-term acceleration. Also, this interface is likely more intuitional relative to "shared control" and more stable due to the above simplification. Furthermore, the bionic hand in the present work is not equipped with tactile feedback; however, the interplay between motor behavior and tactile feedback improves grasping performance, as evidenced by the implanted myoelectric interface [7].

Non-invasive myoelectric prostheses are more popular than implanted prostheses since much safer and more convenient—e.g., taking off it when sleeping [53]. Furthermore, amputees expressed that concerns about myoelectric control are weight, cost, durability, and difficulty of use [53]. The functional benefits of the energy-based myoelectric prostheses seem to consistent with the above concerns. A portable take-home system based on the above technology is developing.

Before ending this paper, it is worth mentioning that the correlation coefficients of off-line analysis are relatively low compared to previous researches in the wrist due to less training data and more DOFs [14-16]. However, because the method is designed by imitating mechanical coupling and physiological coupling of five-fingers in humans, regarding the whole manual task as an energy transfer, subjects can adaptively adjust the energy mode in real-time for the operational experiments, and results are excellent. Moreover, although the learning method we selected, such as ANN or SVM, is similar to previous researches that recorded motions or force of the wrist, the difference of our interface is that we had users perform tasks that represent energy modes in the level of the entire hand. It is very convenient to extend massive manual tasks by training a few energy modes about the entire hand, rather than a lot of motions or single-finger force.

REFERENCES

[1] S. Raspopovic, M. Capogrosso, F. M. Petrini, M. Bonizzato, J. Rigosa, G. Di Pino, J. Carpaneto, M. Controzzi, T. Boretius, E. Fernandez, G. Granata, C. M. Oddo, L. Citi, A. L. Ciancio, C. Cipriani, M. C. Carrozza, W. Jensen, E. Guglielmelli, T. Stieglitz, P. M. Rossini, and S. Micera, "Restoring Natural Sensory Feedback in Real-Time Bidirectional Hand Prostheses," *Science Translational Medicine,* vol. 6, no. 222, pp. 10, Feb, 2014.

[2] B. Peerdeman, D. Boere, H. Witteveen, R. H. in't Veld, H. Hermens, S. Stramigioli, H. Rietman, P. Veltink, and S. Misra, "Myoelectric forearm prostheses: State of the art from a user-centered perspective," *Journal of Rehabilitation Research and Development,* vol. 48, no. 6, pp. 719-737, 2011.

[3] D. Farina, N. Jiang, H. Rehbaum, A. Holobar, B. Graimann, H. Dietl, and O. C. Aszmann, "The Extraction of Neural Information from the Surface EMG for the Control of Upper-Limb Prostheses: Emerging Avenues and Challenges," *Ieee Transactions on Neural Systems and Rehabilitation Engineering,* vol. 22, no. 4, pp. 797-809, Jul, 2014.

[4] D. S. Childress, "CLOSED-LOOP CONTROL IN PROSTHETIC SYSTEMS - HISTORICAL-PERSPECTIVE," *Annals of Biomedical Engineering,* vol. 8, no. 4-6, pp. 293-303, 1980.

[5] M. A. Oskoei, and H. S. Hu, "Myoelectric control systems-A survey," *Biomedical Signal Processing and Control,* vol. 2, no. 4, pp. 275-294, Oct, 2007.

[6] W. W. Lee, Y. J. Tan, H. Yao, S. Li, H. H. See, M. Hon, K. A. Ng, B. Xiong, J. S. Ho, and B. C. K. Tee, "A neuro-inspired artificial peripheral nervous system for scalable electronic skins," *Science Robotics,* vol. 4, no. 32, pp. eaax2198, 2019.

[7] J. A. George, D. T. Kluger, T. S. Davis, S. M. Wendelken, E. V. Okorokova, Q. He, C. C. Duncan, D. T. Hutchinson, Z. C. Thumser, D. T. Beckler, P. D. Marasco, S. J. Bensmaia, and G. A. Clark, "Biomimetic sensory feedback through peripheral nerve stimulation improves dexterous use of a bionic hand," *Science Robotics,* vol. 4, no. 32, pp. eaax2352, 2019.

[8] Ottobock. "Bebionic technical manual," www.ottobockus.com/media/local-media/prosthetics/upper-limb/files/14112_bebionic_user_guide_lo.pdf.

[9] L. McLean, and R. N. Scott, "The Early History of Myoelectric Control of Prosthetic Limbs (1945–1970)," *Powered Upper Limb Prostheses: Control, Implementation and Clinical Application*, A. Muzumdar, ed., pp. 1-15, Berlin, Heidelberg: Springer Berlin Heidelberg, 2004.

[10] P. Parker, K. Englehart, and B. Hudgins, "Myoelectric signal processing for control of powered limb prostheses," *Journal of Electromyography and Kinesiology,* vol. 16, no. 6, pp. 541-548, Dec, 2006.

[11] M. Atzori, M. Cognolato, and H. Muller, "Deep Learning with Convolutional Neural Networks Applied to Electromyography Data: A Resource for the Classification of Movements for Prosthetic Hands," *Frontiers in Neurorobotics,* vol. 10, pp. 10, Sep, 2016.

[12] Y. J. Geng, Y. Ouyang, O. W. Samuel, S. Chen, X. Lu, C. Lin, and G. Li, "A Robust Sparse Representation Based Pattern Recognition Approach for Myoelectric Control," *Ieee Access,* vol. 6, pp. 38326-38335, 2018.

[13] A. Furui, S. Eto, K. Nakagaki, K. Shimada, G. Nakamura, A. Masuda, T. Chin, and T. Tsuji, "A myoelectric prosthetic hand with muscle synergy–based motion determination and impedance model–based biomimetic control," *Science Robotics,* vol. 4, no. 31, pp. eaaw6339, 2019.

[14] N. Jiang, J. L. G. Vest-Nielsen, S. Muceli, and D. Farina, "EMG-based simultaneous and proportional estimation of wrist/hand kinematics in uni-lateral trans-radial amputees," *Journal of Neuroengineering and Rehabilitation,* vol. 9, pp. 11, Jun, 2012.

[15] J. M. Hahne, F. Biessmann, N. Jiang, H. Rehbaum, D. Farina, F. C. Meinecke, K. R. Muller, and L. C. Parra, "Linear and Nonlinear Regression Techniques for Simultaneous and Proportional Myoelectric Control," *Ieee Transactions on Neural Systems and Rehabilitation Engineering,* vol. 22, no. 2, pp. 269-279, Mar, 2014.

[16] S. Muceli, and D. Farina, "Simultaneous and Proportional Estimation of Hand Kinematics From EMG During Mirrored Movements at Multiple Degrees-of-Freedom," *Ieee Transactions on Neural Systems and Rehabilitation Engineering,* vol. 20, no. 3, pp. 371-378, May, 2012.

[17] K. Z. Zhuang, N. Sommer, V. Mendez, S. Aryan, E. Formento, E. D'Anna, F. Artoni, F. Petrini, G. Granata, G. Cannaviello, W. Raffoul, A. Billard, and S. Micera, "Shared human–robot proportional control of a dexterous myoelectric prosthesis," *Nature Machine Intelligence,* vol. 1, no. 9, pp. 400-411, 2019/09/01, 2019.

[18] N. Jiang, K. B. Englehart, and P. A. Parker, "Extracting Simultaneous and Proportional Neural Control Information for Multiple-DOF Prostheses From the Surface Electromyographic Signal," *Ieee Transactions on Biomedical Engineering,* vol. 56, no. 4, pp. 1070-1080, Apr, 2009.

[19] J. R. Napier, "THE PREHENSILE MOVEMENTS OF THE HUMAN HAND," *Journal of Bone and Joint Surgery-British Volume,* vol. 38, no. 4, pp. 902-913, 1956.

[20] C. E. Lang, and M. H. Schieber, "Human finger independence: Limitations due to passive mechanical coupling versus active neuromuscular control," *Journal of Neurophysiology,* vol. 92, no. 5, pp. 2802-2810, Nov, 2004.

[21] C. Hager-Ross, and M. H. Schieber, "Quantifying the independence of human finger movements: Comparisons of digits, hands, and movement frequencies," *Journal of Neuroscience,* vol. 20, no. 22, pp. 8542-8550, Nov, 2000.

[22] H. V. Helmholtz, *The Conservation of Force*, 2003.

[23] M. C. Tresch, P. Saltiel, and E. Bizzi, "The construction of movement by the spinal cord," *Nature Neuroscience,* vol. 2, no. 2, pp. 162-167, Feb, 1999.

[24] L. H. Ting, and J. M. Macpherson, "A limited set of muscle synergies for force control during a postural task," *Journal of Neurophysiology,* vol. 93, no. 1, pp. 609-613, Jan, 2005.

[25] S. A. Overduin, A. d'Avella, J. Roh, and E. Bizzi, "Modulation of muscle synergy recruitment in primate grasping," *Journal of Neuroscience,* vol. 28, no. 4, pp. 880-892, Jan, 2008.

[26] A. d'Avella, A. Portone, L. Fernandez, and F. Lacquaniti, "Control of fast-reaching movements by muscle synergy combinations," *Journal of Neuroscience,* vol. 26, no. 30, pp. 7791-7810, Jul, 2006.

[27] M. R. Cutkosky, "ON GRASP CHOICE, GRASP MODELS, AND THE DESIGN OF HANDS FOR MANUFACTURING TASKS," *Ieee Transactions on Robotics and Automation,* vol. 5, no. 3, pp. 269-279, Jun, 1989.

[28] C. B. Hart, and S. F. Giszter, "Modular premotor drives and unit bursts as primitives for frog motor behaviors," *Journal of Neuroscience,* vol. 24, no. 22, pp. 5269-5282, Jun, 2004.

[29] W. J. Kargo, and D. A. Nitz, "Early skill learning is expressed through selection and tuning of cortically represented muscle synergies," *Journal of Neuroscience,* vol. 23, no. 35, pp. 11255-11269, Dec, 2003.

[30] A. J. Young, L. J. Hargrove, and T. A. Kuiken, "The Effects of Electrode Size and Orientation on the Sensitivity of Myoelectric Pattern Recognition Systems to Electrode Shift," *Ieee Transactions on Biomedical Engineering,* vol. 58, no. 9, pp. 2537-2544, Sep, 2011.

[31] S. Amsuess, P. Goebel, B. Graimann, and D. Farina, "A Multi-Class Proportional Myocontrol Algorithm for Upper Limb Prosthesis Control: Validation in Real-Life Scenarios on Amputees," *Ieee Transactions on Neural Systems and Rehabilitation Engineering,* vol. 23, no. 5, pp. 827-836, Sep, 2015.

[32] "CHAPTER 2 - Anatomy and Kinesiology of the Upper Extremity," *Hand and Upper Extremity Splinting (Third Edition)*, E. E. Fess, K. S. Gettle, C. A. Philips and J. R. Janson, eds., pp. 47-85, Saint Louis: Mosby, 2005.

[33] F. Galis, J. J. M. van Alphen, and J. A. J. Metz, "Why five fingers? Evolutionary constraints on digit numbers," *Trends in Ecology & Evolution,* vol. 16, no. 11, pp. 637-646, Nov, 2001.

[34] R. N. Khushaba, S. Kodagoda, and Ieee, "Electromyogram (EMG) Feature Reduction Using Mutual Components Analysis for Multifunction Prosthetic Fingers Control," *2012 12th International Conference on Control, Automation, Robotics & Vision*, International Conference on Control Automation Robotics and Vision, pp. 1534-1539, New York: Ieee, 2012.

[35] E. D. Engeberg, and S. Meek, "Improved grasp force sensitivity for prosthetic hands through force-derivative feedback," *Ieee Transactions on Biomedical Engineering,* vol. 55, no. 2, pp. 817-821, Feb, 2008.

[36] M. Domalain, L. Vigouroux, F. Danion, V. Sevrez, and E. Berton, "Effect of object width on precision grip force and finger posture," *Ergonomics,* vol. 51, no. 9, pp. 1441-1453, 2008.

[37] A. Sarasola-Sanz, N. Irastorza-Landa, E. Lopez-Larraz, F. Shiman, M. Spuler, N. Birbaumer, and A. Ramos-Murguialday, "Design and effectiveness evaluation of mirror myoelectric interfaces: a novel method to restore movement in hemiplegic patients," *Scientific Reports,* vol. 8, pp. 13, Nov, 2018.

[38] M. Hakonen, H. Piitulainen, and A. Visala, "Current state of digital signal processing in myoelectric interfaces and related applications," *Biomedical Signal Processing and Control,* vol. 18, pp. 334-359, Apr, 2015.

[39] C. C. Chang, and C. J. Lin, "LIBSVM: A Library for Support Vector Machines," *Acm Transactions on Intelligent Systems and Technology,* vol. 2, no. 3, pp. 27, 2011.

[40] J. L. G. Nielsen, S. Holmgaard, N. Jiang, K. B. Englehart, D. Farina, and P. A. Parker, "Simultaneous and Proportional Force Estimation for Multifunction Myoelectric Prostheses Using Mirrored Bilateral Training," *Ieee Transactions on Biomedical Engineering,* vol. 58, no. 3, pp. 681-688, Mar, 2011.

[41] J. M. Hahne, M. A. Schweisfurth, M. Koppe, and D. Farina, "Simultaneous control of multiple functions of bionic hand prostheses: Performance and robustness in end users," *Science Robotics,* vol. 3, no. 19, pp. 9, Jun, 2018.

[42] K. J. Cole, and D. L. Rotella, "Old age impairs the use of arbitrary visual cues for predictive control of fingertip forces during grasp," *Experimental Brain Research,* vol. 143, no. 1, pp. 35-41, Mar, 2002.

[43] C. Voelcker-Rehage, A. J. Stronge, and J. L. Alberts, "Age-related differences in working memory and force control under dual-task conditions," *Aging Neuropsychology and Cognition,* vol. 13, no. 3-4, pp. 366-384, Sep-Dec, 2006.

[44] C. Choi, and J. Kim, "Synergy matrices to estimate fluid wrist movements by surface electromyography," *Medical Engineering & Physics,* vol. 33, no. 8, pp. 916-923, Oct, 2011.

[45] N. Jiang, H. Rehbaum, I. Vujaklija, B. Graimann, and D. Farina, "Intuitive, Online, Simultaneous, and Proportional Myoelectric Control Over Two Degrees-of-Freedom in Upper Limb Amputees," *Ieee Transactions on Neural Systems and Rehabilitation Engineering,* vol. 22, no. 3, pp. 501-510, May, 2014.

[46] A. Hyvarinen, and E. Oja, "Independent component analysis: algorithms and applications," *Neural Networks,* vol. 13, no. 4-5, pp. 411-430, May-Jun, 2000.

[47] N. Jiang, I. Vujaklija, H. Rehbaum, B. Graimann, and D. Farina, "Is Accurate Mapping of EMG Signals on Kinematics Needed for Precise Online Myoelectric Control?," *Ieee Transactions on Neural Systems and Rehabilitation Engineering,* vol. 22, no. 3, pp. 549-558, May, 2014.

[48] N. Jiang, S. Dosen, K. R. Muller, and D. Farina, "Myoelectric Control of Artificial Limbs-Is There a Need to Change Focus?," *Ieee Signal Processing Magazine,* vol. 29, no. 5, pp. 147-150, Sep, 2012.

[49] K. Englehart, B. Hudgins, and P. A. Parker, "A wavelet-based continuous classification scheme for multifunction myoelectric control," *Ieee Transactions on Biomedical Engineering,* vol. 48, no. 3, pp. 302-311, Mar, 2001.

[50] Z. Y. Lu, K. Y. Tong, X. Zhang, S. Li, and P. Zhou, "Myoelectric Pattern Recognition for Controlling a Robotic Hand: A Feasibility Study in Stroke," *Ieee Transactions on Biomedical Engineering,* vol. 66, no. 2, pp. 365-372, Feb, 2019.

[51] Y. Zhou, Y. F. Fang, K. Gui, K. R. Li, D. G. Zhang, and H. H. Liu, "sEMG Bias-Driven Functional Electrical Stimulation System for Upper-Limb Stroke Rehabilitation," *Ieee Sensors Journal,* vol. 18, no. 16, pp. 6812-6821, Aug, 2018.

[52] D. Leonardis, M. Barsotti, C. Loconsole, M. Solazzi, M. Troncossi, C. Mazzotti, V. P. Castelli, C. Procopio, G. Lamola, C. Chisari, M. Bergamasco, and A. Frisoli, "An EMG-Controlled Robotic Hand Exoskeleton for Bilateral Rehabilitation," *Ieee Transactions on Haptics,* vol. 8, no. 2, pp. 140-151, Apr-Jun, 2015.

[53] S. M. Engdahl, B. P. Christie, B. Kelly, A. Davis, C. A. Chestek, and D. H. Gates, "Surveying the interest of individuals with upper limb loss in novel prosthetic control techniques," *Journal of Neuroengineering and Rehabilitation,* vol. 12, pp. 11, Jun, 2015.